



A MATERIAL AND STRUCTURAL ANALYSIS OF EARTHBAG HOUSING

Student: Nikul Vadgama
Supervisor: Dr. Andrew Heath
MEng Dissertation

April 2010

Abstract

The use of earthbags as structural material for housing has grown in popularity over the past decade; however, research into its structural behaviour is limited. Current design relies on previous experience or trial and error. If the use of earthbags as building material is to develop, an understanding into its material properties and structural behaviour is needed. By way of empirical analysis this dissertation aims to investigate the material mechanics of sand filled earthbags and establish a set of material parameters which will aid the design of earthbag structures.

The dissertation is collaborative with Fielden Clegg Bradley Studios who plan to build earthbag housing in Namibia. Test parameters for this dissertation have been chosen specifically to help inform the project, which in turn provides a physical bearing to the experimental programme and analysis.

The behaviour of earthbags under uniaxial compression was investigated. The effect of material fill level, stack height, addition of stabiliser and bag material on the compressive strength were explored. From testing it was concluded that earthbags are unlikely to fail due to compression within a structure. Furthermore the current simplified theoretical model assuming a cross section with lateral semi-circular profiles provides acceptably accurate estimations of the vertical load capacity of earthbags.

Large scale direct shear box tests were performed to quantify the shear resistance between earthbags. Variations in bag material and the inclusion of barbwire were examined. A hessian on hessian interface provided the highest coefficient of friction. The inclusion of barbwire also improved the coefficient of friction between the earthbags are provided an initial cohesion.

Load testing on earthbag arches were performed to gain an understanding how the material parameters affect the structural performance. The addition of 4% cement to the earthbags was found to increase the load capacity of the arch by 76% and alter the overall behaviour of the arch to a linear elastic structure up to 6kN applied load. The behaviour of an unstabilised arch is non-linear, owing to the flexible nature of the bags. Premature shear failure of the earthbags was not experienced therefore the addition of barbwire between bags did not affect the load capacity of the arch.

This dissertation provides an insight into the material and structural behaviour of earthbags. To further establish a set of structural parameters for design, research into the behaviour of earthbags in defined structural systems should be undertaken.

Acknowledgements

The author would like to acknowledge the invaluable support and guidance provided by Dr. Andrew Heath during the course of this dissertation, and throughout the author's undergraduate degree.

Gratitude also extends to Will Bazeley, Neil Price, Brian Purnell, and Sophie Hayward for their time and expertise with laboratory experiments.

Also thanks extend to Nicola du Pisanie for her enthusiasm and advice throughout the dissertation. For his assistance with laboratory experiments, organisation and motivational work ethic the author thanks Ralph Pelly.

Finally, to my family and friends for their support throughout.

Contents

Abstract.....	i
Acknowledgements.....	ii
List of Figures.....	v
List of Tables.....	vii
List of Symbols and Abbreviations.....	vii
1 Introduction.....	1
1.1 General Introduction.....	1
1.2 Objective of Dissertation.....	2
1.3 Organisation of Dissertation.....	2
2 Namibia Project.....	3
3 Literature Review.....	4
3.1 Introduction to Literature Review.....	4
3.2 Previous Research into Earthbags.....	4
3.3 Summary of Literature Review.....	9
4 Theory.....	11
4.1 Initial Conditions and Assumptions.....	11
4.2 Compressive Strength of Earthbags.....	11
4.2.1 Assuming earthbag cross section as rectangular.....	12
4.2.2 Assuming earthbag cross section with semi-circular lateral edges.....	14
4.2.3 Summary of theoretical compressive strength of earthbag.....	16
4.3 Shear Strength of Earthbags.....	17
4.4 Theoretical Earthbag Arch Mechanism.....	18
5 Laboratory Testing.....	20
5.1 Soil Analysis.....	20
5.1.1 Sieve Test.....	20
5.1.2 Shear Box Tests.....	20
5.2 Tensile Tests on Bag Material.....	20
5.3 Compression Tests.....	20
5.4 Shear Tests.....	22
5.5 Arch Test.....	23
5.5.1 Stabilised Arch Tests.....	24

6	Results & Analysis.....	25
6.1	Soil Analysis.....	25
6.1.1	Sieve Tests.....	25
6.1.2	Shear Box Tests.....	25
6.2	Tensile Test on Bag Material.....	26
6.3	Compression Tests.....	27
6.3.1	Three earthbag stack.....	27
6.3.2	Five earthbag stack.....	30
6.3.3	Eight earthbag stack.....	30
6.3.4	Comparison between experimental results with theoretical predictions.....	33
6.3.5	Sources of error in experimental and theoretical work.....	36
6.3.6	Summary and conclusion of compression tests.....	37
6.4	Shear Test of Earthbags.....	38
6.4.1	Shear resistance in earthbag structures.....	41
6.5	Arch Test.....	44
6.5.1	Earthbag arches loaded at quarter span.....	45
6.5.2	Summary and conclusion of earthbag arch tests.....	48
7	Conclusion.....	49
7.1	Future Work.....	50
	Bibliography.....	51
	Appendix A.....	53
	Appendix B.....	54
	Appendix C.....	55
	Appendix D.....	59
	Appendix E.....	60

Appendices can be found in accompanying C.D.

List of Figures

Figure 1: Construction of earthbag domes by Cal-Earth (Cal-Earth Inc. / Geltaftan, 2010).	1
Figure 2: Aluminium rods wrapped in Japanese paper under compression (Matsuoka & Liu, 2003).....	4
Figure 3: Variation in tensile stress in the bag material for an interlock interface with different vertical displacements, found from finite element model (Tantono, 2007).	5
Figure 4: Apparatus for biaxial compression test on 2D model earthbags and variation of the apparent cohesion of the inclined earthbags $c(\delta)$, where δ is angle of inclination (Matsuoka & Liu, 2003).	6
Figure 5: Earthbag pile before and after compression test, showing global shear band (Lohani <i>et al.</i> , 2006).	7
Figure 6: Free body diagram a) vertically and b) horizontally through earthbag under uniform vertical loading.	13
Figure 7: Mohr’s Circle showing failure envelope of the earthbag where $\sigma_v > \sigma_h$	13
Figure 8: Free body diagram a) vertically and b) horizontally through earthbag with lateral semi-circular edges.	15
Figure 9: Mohr’s circle showing the affect of the application of cement on granular fill.	16
Figure 10: Theoretical failure mode of barbwire under direct shear a) overall view b) failure by bending c) rigid body shear failure.	18
Figure 11: Force equilibrium about barbwire point showing lateral resistance of soil against applied lateral force from the soil and bag material.	18
Figure 12: Arrangement for eight earthbag stack compression tests	21
Figure 13: Earthbag shear test apparatus	22
Figure 14: Arch test apparatus	24
Figure 15: Shear box test; shear stress at failure against effective stress normal to the failure plane.	25
Figure 16: Stress strain relationship from tensile tests of all bag material samples.....	26
Figure 17: Compression test results of three 100gsm polypropylene earthbags with varying amount of fill.	28
Figure 18: Three earthbag 100gsm polypropylene stack compression test showing enlarged section of load displacement graph.	29
Figure 19: Stress strain relationship of earthbags in compression, with variation in stack height	30
Figure 20: Location of transducers, failure points in bag material and recover of earthbag stack after unloading	31
Figure 21: Load displacement graph for eight stabilised 100gsm polypropylene, unstabilised 100gsm polypropylene and unstabilised 70gsm polypropylene earthbags.	31
Figure 22: Tearing of 70gsm polypropylene earthbags after compression test	32
Figure 23: Ratio of measured volume of earthbag in 8 bag stack to initial volume of earthbag against displacement of platen	35
Figure 24: Shear strength against normal compressive stress for large shear box experiment with variation in interface between earthbags.	38
Figure 25: Interface between hessian earthbags after large shear box test	39
Figure 26: Image of earthbag showing points where bag material was torn during direct shear test.	40
Figure 27: Predicted shear failure mode of earthbags in a dome structure subject to a line load.	41

Figure 28: Comparison between shear resistance due to friction between earthbags and due to barbwire mechanism in a hemispherical dome.	43
Figure 29: Picture of earthbag and abutment for first unstabilised earthbag arch test.....	45
Figure 30: Photos from stabilised arch test showing hinge mechanism failure of arch.....	47
Figure 31: Masonry arch analysis using Ring 2.0.....	47
Figure 32: Load displacement graph for earthbag arches loaded at quarter span	48
Figure 33: Dry sieve analysis of Kuiseb riverbed sand, near Gobabeb.	53
Figure 34: Dry sieve analysis builders sand - Bath.....	53
Figure 35: Diagram showing how earthbags were measured.	54
Figure 36: Large scale shear box test for 100gsm polypropylene earthbag no barbwire - 2.2kN applied normal load	55
Figure 37: Large scale shear box test for 100gsm polypropylene earthbag no barbwire - 7.1kN applied normal load	55
Figure 38: Large scale shear box test for 100gsm polypropylene earthbag no barbwire - 12.0kN applied normal load	56
Figure 39: Large scale shear box test for 100gsm polypropylene earthbag no barbwire - 17.0kN applied normal load	56
Figure 40: Large scale shear box test for 100gsm polypropylene earthbag with barbwire - 2.2kN applied normal load	57
Figure 41: Large scale shear box test for 100gsm polypropylene earthbag with barbwire - 7.1kN applied normal load	57
Figure 42: Large scale shear box test for 100gsm polypropylene earthbag with barbwire - 12.0kN applied normal load	58
Figure 43: Large scale shear box test – hessian earthbags.....	58
Figure 44: Change in perimeter over initial perimeter of 70gsm polypropylene earthbag in 8bag compression test against normalised displacement of loading platen.....	59
Figure 45: Single earthbag in hemisphere dome showing contact forces	60

List of Tables

Table 1: Tensile strengths of all bag material samples obtained from tensile tests.....	26
Table 2: Summary of earthbag compression test results	33
Table 3: Comparison between measured bag width with theoretical bag width at failure load.....	34
Table 4: Comparison between theoretical vertical deformation and experimental vertical deformation of an earthbag.....	35
Table 5: Comparison between theoretical and experimental failure loads of the earthbags under vertical compression.....	36
Table 6: Horizontal displacement at which shear strength was mobilised.....	38
Table 7: Summary of results from earthbag arch tests.....	44
Table 8: Earthbag dimensions and densities for compression tests.....	54
Table 9: Moisture content of sand for barbwire and stabilised arch tests.....	54

List of Symbols and Abbreviations

μ	Coefficient of friction
ϕ	Internal friction angle of material fill
σ_h	Horizontal stress exerted by soil onto the bag material
σ_{bag}	Tensile stress in bag material
σ_{bag}^{limit}	Limit tensile stress in bag material
σ_v	Vertical stress exerted by the soil onto the bag material
B_0, B	Initial width and current width of earthbag
E	Elastic modulus of bag material
H_0, H	Initial height and current height of earthbag
K	Stress ratio in the soil inside the earthbag
L_0, L	Initial perimeter and current perimeter of earthbag
P_a	Axial force in barbwire point
P_s	External direct shear force
P_T	Tension force in barbwire strand
p_v	External applied vertical pressure
P_v	External applied vertical load
t	Thickness of bag material
T	Tension force in bag material
V_0, V	Initial volume and current volume of earthbag
x	Vertical deformation of earthbag
FCBS	Fielden Clegg Bradley Studios
LVDT	Linear variable displacement transducer

1 Introduction

1.1 General Introduction

The issue of sustainability in the built environment can be defined in a variety of ways; Kibbert (1994) expresses it as: *'The creation and management of a healthy built environment based on resource efficient and ecological parameters.'* Sustainable design requires an efficient, intelligent use and allocation of our natural resources, which must be balanced with social and economic criteria. Often the economic criterion governs, leading to unsustainable design focused primarily on short term needs. Much of the developing world live in poor housing due to a lack of economic support, limited resources and/or a lack of construction knowledge. There is no forthright solution, however in many cases; particularly rural areas where resources are limited, earthbag construction offers many benefits.

Earthbags (also known as soilbags or sandbags) are polymer material or burlap (hessian) bags filled with granular materials. The application of earthbags is long been used as temporary construction. Its use as flood protection and military walls is well established; however, its use as permanent structure has been growing in popularity. As well as material for housing, earthbags have been used as facing for reinforced soil retaining walls and to increase the bearing capacity of footings. Earthbag housing usually consists of earthbags stacked in a corbelled fashion to create a catenary dome, with layers of barbwire between courses to provide shear resistance.



Figure 1: Construction of earthbag domes by Cal-Earth (Cal-Earth Inc. / Geltaftan, 2010).

Exploration into earthbag housing can be dated back to the 1970's and the work of Gernot Minke. Minke's research explored fabric bags filled with pumice used in corbelled shaped domes. However, it was the work of Nader Khalili and his organisation Cal-Earth who popularised the use of earthbags as structural material for housing. Khalili used barbwire between courses to provide tensile strength to the structure and allows shear transfer between courses.

Earthbag construction is suited for developing countries given it is economic, does not require any large processes or highly skilled construction labour, the materials required are easily attainable and the construction process is relatively quick. These attributes also make earthbag construction ideal for disaster relief housing. With earthbag housing the surrounding soil can be used to fill the bags, hence making the construction technique efficient and sustainable.

1.2 Objective of Dissertation

Although the construction method for earthbag housing is well developed, the understanding and research into the mechanical behaviour of earthbags and failure modes of earthbag structures is not. If the application of earthbags for housing is to develop, then further structural and material analysis of earthbag structures must take place to give confidence to construct with earthbags. The aim of this dissertation is to investigate the material mechanics of earthbags to establish a set of material properties needed for structural analysis of earthbag housing. This will be achieved through a series of experiments and analysis into the soil properties, bag properties, earthbag structural properties and effects from stabilisation of the earthbags. A full description of the laboratory experiments undertaken is given in §5.

This research was undertaken in conjunction with Pelly (2010), whose dissertation explores using the material properties to investigate the geometrical limitations of earthbag structures.

1.3 Organisation of Dissertation

Chapter 2: Outline of proposed project in Namibia, building sandbag structure housing for the Topnaar community and how this project relates to the dissertation.

Chapter 3: A review of literature relevant to earthbag housing and the properties of earthbags has been undertaken to establish current knowledge on the subject and areas that can be further explored.

Chapter 4: Explanation of theoretical modelling of earthbag structures for compression, shear and arch tests.

Chapter 5: Description of experimental procedure used for soil analysis, compression, shear and arch tests.

Chapter 6: Presentation of results from experimental programme and analysis of the results with respect to theoretical predictions.

Chapter 7: Conclusions from experiments and proposal for further investigation is outlined.

2 Namibia Project

Earthbag structures are generally explicit to their surrounding conditions. The material fill is often taken directly from the ground the structure is based and the bag material varies to whatever is attainable. Hence, each project can only rely so much on previous experience; a further fundamental understanding of material behaviour is required to aid design. Given the variability of materials employed a defined scope was needed to narrow the potential research areas of this dissertation.

The dissertation is collaborative with Fielden Clegg Bradley Studios who are working to construct earthbag dome structures in Gobabeb, Namibia. This connection with the project has helped direct test parameters and provide tangible relevance to the results from this dissertation. The aim of the Namibia project is to introduce the earthbag construction technique to the local Topnaar community through a prototype build, which the Topnaar can independently use for their own homes if they wish.

Currently the majority of the Topnaar live in salvaged timber frame houses with corrugated metal sheet cladding. The houses have no real thermal resistance, hence are very hot during summer (recorded 5-7°C hotter internally than externally (du Pisanie, 2009)) and extremely cold during the colder spells. FBCS look to introduce a building technique which was more suited to the desert climate. Earthbag housing was selected as it provides high thermally mass, thus is less susceptible to diurnal temperature fluctuations. In addition all the materials can be easily sourced; the fill itself can be taken from the nearby river plain. It is very quick to build and can be built with mainly unskilled labour, with one or two experienced people co-ordinating. The construction requires a large workforce, thus will require the whole community to participate. FCBS hope this will bring the community together and implement the building technique across the community.

To relate to the build in Namibia this paper has only considered fine sand with no clay content as fill; hence replicated something similar to that found in Gobabeb, Namibia (see Appendix A). Varying the clay content will affect the cohesion of the fill, and potentially provide a more rigid block. However, each variation of clay content would need to be tested for the compression, shear and arch tests. This quantity of testing is unrealistic in the time frame of this dissertation, hence is not considered. A stabilised case has been considered for the arch and compression tests, to improve the stiffness of the earthbag, as this is a viable option for the Gobabeb project. Finally, no earthbags over 20kg will be tested as a weight over this amount becomes difficult to manoeuvre in construction.

3 Literature Review

3.1 Introduction to Literature Review

A literature review was undertaken to establish current understanding of earthbag structures and how previous research has approached the subject both experimentally and analytically. As previously mentioned in §1.2 to establish a design practice for earthbag structures a greater understanding of their material properties and structural failure modes is needed. From the literature review it was found that previous material analysis on earthbags as building material is limited, however, analysis in relation to their use as earth reinforcement has been investigated. Experimental research into the compressive and shear strength of earthbags has been undertaken and is discussed in the following chapter.

3.2 Previous Research into Earthbags

Matsuoka & Liu, 2003 investigated the application of earthbags as '*reinforcement for ballast foundations under railway sleeper, reinforcement for soft building foundations and construction of retaining walls*'. Early 2D models consisted of bearing tests on 50mm long aluminium rods, which had a specific gravity G_s of 2.69 similar to that of soil particles (2.65) (Matsuoka & Liu, 2003). The aim of the experiments was to improve the bearing capacity of the rods by use of Japanese paper as reinforcement. Load was applied to the rods via a footing (Figure 2). The paper was used as tensile reinforcement and wrapped around the aluminium rods thereby producing a stiff region within which relatively less deformation occurs, furthermore the region underwent movement concurrent with the footing as shown in Figure 2. The vertical load applied causes the aluminium rods to push outward which induces a tensile force into the paper; this in turn exerts an equal and opposite stress to the rods. It was found that this model can be applied to earthbags and analysed with a Mohr-Coulomb failure criterion to give the failure load of earthbags which is outlined later in this paper. Significantly, Matsuoka & Liu (2003) outlined that the compressive capacity of the earthbag is limited by the tensile capacity of the bag material. Hence if the tensile capacity of the bag material is known, from a Mohr-Coulomb failure envelope, the external compressive force which causes failure can be deduced.

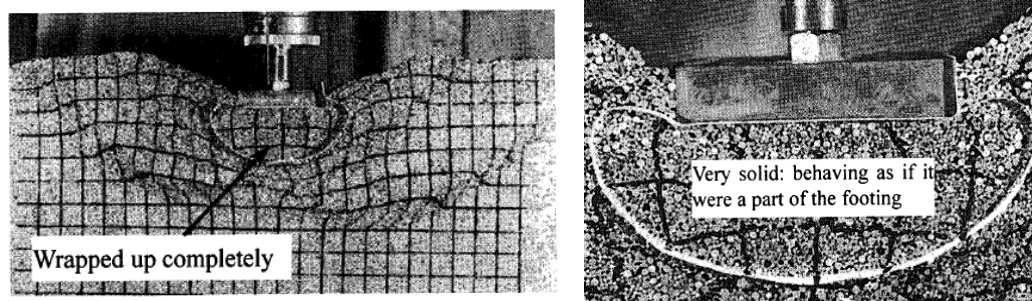


Figure 2: Aluminium rods wrapped in Japanese paper under compression (Matsuoka & Liu, 2003).

Matsuoka & Liu (2003) verified the theoretical analysis of the strength properties of earthbags with biaxial compression tests on aluminium rods wrapped in paper. These 2D experiments were useful to support the theoretical analysis however are limited in that they do not consider the 3D confining effect; thus in reality earthbags will exhibit a higher strength than the theory suggests. Furthermore the analysis assumes a frictionless interface between the bag material and the fill. This is not true, there is likely to be some particle interlock at the interface and the distribution of shear deformation vertically through the earthbag is non linear. Furthermore the tensile force in the bag varies across the section contrary to the assumption made by Matsuoka & Liu (2003). From previous compression test (e.g. Lohani *et al.*, 2006; Matsuoka & Liu, 2003 and Xu *et al.*, 2008) the earthbags tend to fail at the top and bottom faces, thus, it is fair to conclude that the horizontal stresses can be considered to cause the bag material to reach its tensile capacity and no vertical confinement is provided by the bag. This is further support by finite element analysis undertaken by Tantonio (2007) considering particle interlock at the interface, which indicated that the tensile stresses in the middle of the bag material were high than at the edges (see Figure 3). Furthermore this assumption would satisfy vertical equilibrium given $p_v = \sigma_v$, this model has been further explored in §4.2.1.

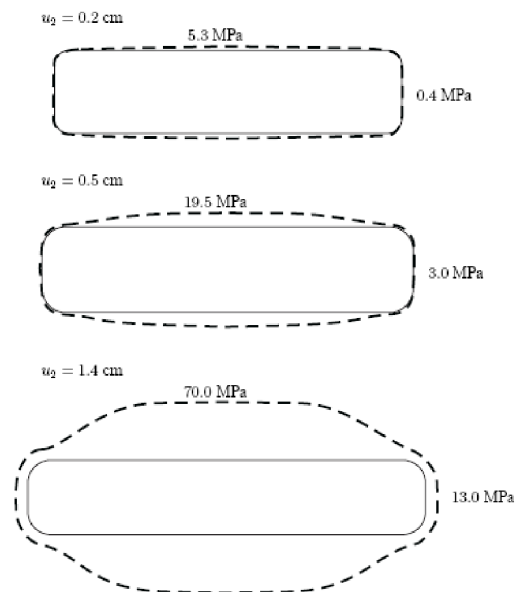


Figure 3: Variation in tensile stress in the bag material for an interlock interface with different vertical displacements, found from finite element model (Tantonio, 2007).

In reality earthbags are likely to be loaded in various directions, Matsuoka & Liu (2003) investigated the effect of inclined loads on the apparent cohesion of the earthbag using biaxial compression tests, see Figure 4. The earthbags were inclined at 0° , 15° , 30° , 45° , 60° and 90° to the load (Matsuoka & Liu, 2003). It was found that the apparent cohesion provided by the bag reduces as the load inclination tends to 45° , where after it is 0. This is important when considering earthbags in a dome structure where the load is inclined according to the thrust line,

through a section of the dome. Hence if the rise of the dome is lowered, apparent cohesion provided by the bags and hence the compressive strength of the bags is reduced.

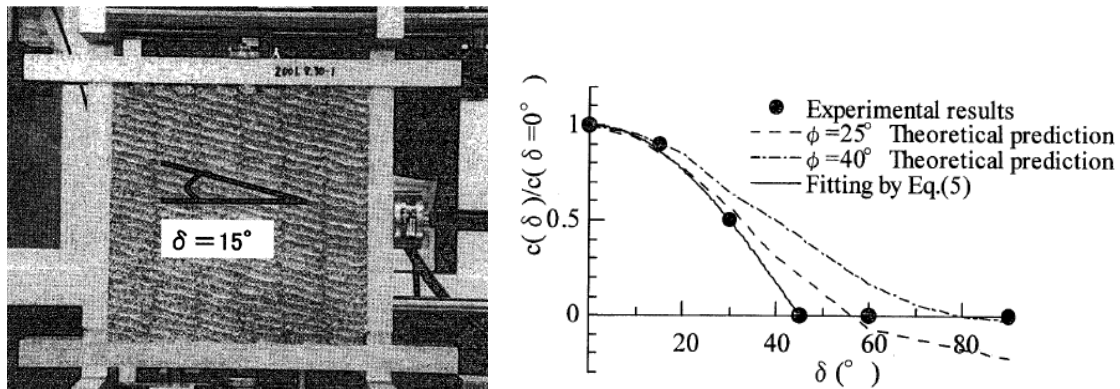


Figure 4: Apparatus for biaxial compression test on 2D model earthbags and variation of the apparent cohesion of the inclined earthbags $c(\delta)$, where δ is angle of inclination (Matsuoka & Liu, 2003).

Unconfined compression tests on earthbags were carried out by Matsuoka & Liu, (2003) with various bag materials and fills although it is unclear exactly what bag materials were used as conflicting information is given in the paper. The bag deformation was not recorded throughout loading, thus the predicted failure loads are made with initial bag dimensions and as such were lower than actual values. Furthermore no initial study on soil properties was undertaken, so no experimental analysis into the failure load of the soil was undertaken.

Three bags were loaded at one time to reduce the effect of friction on the upper and lower ends of the loading unit (Matsuoka & Liu, 2003). However, this would not be sufficiently high to remove end restraint effects and hence lead to an overestimation of the earthbag strength and inhibits a global shear band developing as noted by Lohani *et al.* (2006).

Lohani *et al.* (2006) conducted several experiments on the compressive and shear strength of an earthbag pile. The study focuses on the application of earthbags for permanent civil engineering structures. Like Matsuoka & Liu (2003), Lohani *et al.* (2006) concluded that the compressive strength of the earthbag is limited by the rupture of the bag material. However, for the compression tests, lateral deformation of the earthbags was recorded using 16 pulley type LVDTs attached to the earthbags (Lohani *et al.*, 2006). Hence analysis by Lohani *et al.* (2006) used the deformed shape of the bag to calculate the earthbags' compressive strength, rather than initial values like Matsuoka & Lin, (2003) which underestimates the axial force required to cause failure of the bag. A vibratory compactor was used to compact the earthbags; however, a hand tamper has been used for this project given that this would be more likely used in the construction of an earthbag house.

From the conducted axial compression tests by Lohani *et al.* (2006), four earthbags reach the maximum capacity of the machine. Lohani *et al.* (2006) deduced that this was an overestimation

of the compressive strength and is due to the end restraint effects which are more apparent at low ratios of height to width (H/B) of the pile. At low H/B ratios the bags are under additional confinement at the ends, which prohibits lateral expansion of the bags and induces shear stress. Thus compressive testing was also undertaken on earthbag piles with an H/W ratio ≥ 2 . Figure 5 shows an earthbag pile with H/B = 2.43 (Lohani *et al.*, 2006); it can be seen that lateral strains reached the failure strain limit of the bag material, furthermore that a global shear band was able to develop. For the compression tests undertaken by Matsuoka & Lin (2003) the H/W ratio was measured to be 0.75, hence the effect of end restraint was higher leading to an overestimating of the compressive strength.

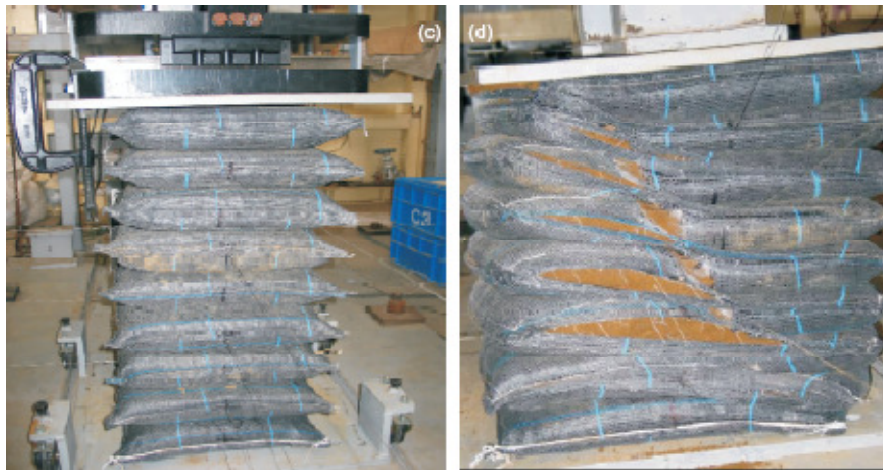


Figure 5: Earthbag pile before and after compression test, showing global shear band (Lohani *et al.*, 2006).

Lateral shear tests were performed on 2 piles consisting of 4 earthbags. The top platen was moveable and the two piles were laterally in contact. A normal load was applied to the piles and a constant shear rate of 0.3mm/min was maintained (Lohani *et al.*, 2006). It was found that mobilisation of shear strength of the fill was higher in compression tests than in lateral shear tests. Furthermore, the earthbag exhibited high anisotropic strength, due to the bags not being laterally confined, which resulted in negligible complementary shear developed between the vertical bag piles. Lohani *et al.* (2006) concluded that this indicated the stress distribution within the bags was non-uniform, which ‘*results in a dominant overturning displacement mode of the soil bag piles and therefore a low shear strength with highly contractive behavior*’ (Lohani *et al.*, 2006). The angle of the major principal stress is inclined, according to the ratio of vertical to horizontal force. Given the high anisotropic behaviour exhibited in these tests, it can be shown that as the inclination of the resultant compressive load increases towards 45°, a state of pure shear, the shear strength of earthbag piles greatly reduces. This is supported by Matsuoka & Liu (2003), and highlights the importance of barbwire to transfer shear between earthbag courses.

Tantono (2007) extended the analytical model of Matsuoka & Liu (2003) and outlines numerical simulations for the mechanical behaviour of earthbags under vertical compression for plane

strain condition. The analytical method made similar assumptions to Matsuoka & Liu (2003) some of which are outlined in §4.1. From analytical analysis Tantonno (2007) proved that the ratio of perimeter to initial perimeter of the earthbag varies non-linearly with ratio of vertical displacement of platen to the initial height of the earthbag. Hence for large axial strains the assumption that the earthbag deforms under vertical load with constant volume does not hold true, however at small strains it is fairly accurate. Tantonno (2007) analytically showed that an increase in the stress ratio ($K = \sigma_v/\sigma_h$), which is related to the critical friction angle of the soil, provides a stiffer earthbag with a higher compressive capacity. This indicates that theoretically a material fill with a higher friction angle will provide an earthbag with a high compressive strength, however, as shown by Daigle (2008) experimentally this does not hold true (see page 9).

Tantonno (2007) identified that the proposed analytical model by Matsuoka & Liu (2003) did not satisfy local equilibrium close to the top and bottom of the earthbag, given the applied stress (p_v) does not equal the stress in the material (σ_v). Tantonno (2007) proposed a new model with lateral semicircular ends which satisfies both global and local equilibrium. In this model the stress ratio is not assumed to be constant, the middle part of earthbag has a stress ratio $K = 3$, while the semicircular areas have $K = 1$ (Tantonno, 2007). It was found that the contribution of vertical stress in the soil at the semicircular area provided local vertical equilibrium. Furthermore, in comparison with the Matsuoka & Liu (2003) model, the Tantonno (2007) model produces a higher stress in the bag for a vertical displacement, therefore failure occurs at a lower vertical load. This can be attributed to the different distributions of stress ratio chosen by the two models. In this dissertation the Tantonno (2007) model will be examined in relation to the experimental data from vertical compression tests to assess its accuracy.

As previously outlined the analytical models assume a constant volume throughout loading, however this does not hold for larger axial strains and finite element analysis could be used. An adopted micro-polar continuum approach by Bauer & Huang (1999) is used to numerically model the granular material within the bag. The model considers Cosserat rotations (local particle rotations), sliding at the interface, void ratio, normal, shear and couple stresses (torque per unit area). The equations for Cauchy stress tensor and couple stress tensor are incrementally non-linear and considered with respect to hypoplasticity (Huang & Bauer, 2003).

The numerical analysis considered two scenarios, a frictionless and an interlock interface between the soil and the bag. The frictionless model allowed local particle rotations and sliding at the interface. It was found that the tensile stress in the bag is uniform; however, the stress ratio inside the bag is inhomogeneous (Tantonno, 2007). The stress ratio in the middle of the bag was higher than at the side, in the hypoplastic material model, and with an increase in vertical displacement tends towards $K = 3$. The stress ratio at the lateral boundary was close to one; hence verifying the assumptions for the simplified semi-circular model. Strain localisation occurred at the points where the voids ratio is higher. The shear band thickness, location and orientation are

dependent upon the microstructure (mean grain size), vertical pressure, boundary conditions and current state of the material (Roscoe, 1970).

From Tantonno (2007) the numerical model with interlocked interface had a non uniform tensile stress distribution in the bag material (see Figure 3); this is a more representative model of the earthbag under vertical loading. The stresses were higher in the middle of the earthbag than at the sides; furthermore the stress limit of the bag was reached earlier with the interlocked interface than the frictionless. Hence, the load capacity of the earthbag with an assumed interlock interface is lower than a frictionless. Unlike the frictionless model, no significant strain localisation was experienced in the soil and the centre of the soil remained mainly in compression.

From extensive research, Daigle (2008) currently provides the only structural investigation into the direct application of earthbags as structural material for housing. Daigle (2008) considers the structural behaviour of earthbags under vertical compressive loads, concentrating on producing a standard testing procedure. Three fill materials were considered, crushed granite, topsoil and Kingston topsoil with masonry sand. Crushed granite, although has the highest friction angle, produced the lowest compressive strength earthbags, which can be attributed to the sharp corners of the granite aggregate rubbing against the bag, causing the bag to tear.

Tensile tests on polypropylene bags were undertaken using a wide strip method according with ASTM D 4595. Narrow strip method was avoided as the influence of edge effects (i.e. bowing of the sample due to server Possion's ratio effects (Daigle, 2008; Koerner, 1997) along the sides is higher.

The paper provided a greater understanding of the behaviour of various fill materials. However, only the granite reached failure, the other two reached the capacity of the loading machine, thus their ultimate capacity is unknown. Too few material fills were considered for a valuable quantitative analysis on the affect of material fill on the compressive strength of earthbags. Both the topsoil and Kingston topsoil with masonry sand consisted of over 25% clay and silts; a further analysis could have been undertaken to assess the effect of clay content on the stiffness of earthbags. The outlined methodology for compression testing is simple to follow, however, offers nothing new from previous research (e.g. Matsuoka & Liu, 2003; Lohani *et al.*, 2006; Xu *et al.*, 2008).

3.3 Summary of Literature Review

Current research from Matsuoka & Liu (2003) and Tantonno (2007) provides good analytical models for the mechanics of earthbags under vertical compression. Furthermore Tantonno (2007) supplemented his analytical model with a FEM model; however, this model has only been applied to small displacements, therefore may not be entirely accurate for the experiments. Furthermore both analytical models consider a frictionless interface between the bag and the fill which is unrealistic. The analytical models and the results from the numerical model will be

verified with experimental data from this paper. Lohani *et al.* (2006) presented the importance of end restraints, in over estimating the strength of earthbags, thus some compression tests will have $H/W > 2$. The paper also demonstrates the poor shear strength of earthbags when subjected to an inclined load. This will be further explored in this paper which attempts to quantify the shear strength between earthbags from an in plane load. Current engineering literature on the earthbags only considers their application in a vertical retaining wall situation. This dissertation will give a material analysis of earthbag housing; furthermore will investigate the material mechanics of earthbags in relation to dome / arch geometries.

4 Theory

4.1 Initial Conditions and Assumptions

The following assumptions are made for analysis of the behaviour of earthbags for the various loading cases:

- The earthbags have a constant cross section and are completely filled with a cohesionless granular material; the volume of the bags do not change throughout loading. The earthbags have a rectangular cross section for the shear and arch tests; however, for the compression test lateral semi-circular boundaries will also be considered.
- For the compression test, the platens are rigid and parallel. Furthermore the surface of the platen is frictionless.
- The behaviour of the bag material is linear elastic and remains constant thickness throughout loading.
- Plane strain condition.
- Earthbag will fail at the top and bottom face hence the bag material reaches tensile capacity only at these points.
- For an uncompressed state there is no stress induced in the bag material or material fill, the weight of the fill material is neglected.
- The stress ratio σ_v/σ_h is assumed to be constant throughout loading.

4.2 Compressive Strength of Earthbags

When subject to an external vertical load the bag material provides confinement to the fill which induces a tension in the bag material. Failure occurs when there is a loss in confinement provided, i.e. when the bag material is stressed to its stress limit.

In reality the earthbags will not maintain a uniform rectangular section, there is likely to be localised deformations thus the contact area between the platen and bags and between the bags will be non uniform. Furthermore there will be significant friction at the interface between the platen and earthbag, which would mean a proportion of the applied load will be taken by the platen hence leading to an artificially high compressive strength.

The interface between the bag material and the soil will not be frictionless and the boundary will affect the deformation behaviour of the sand, particularly at high vertical stresses. Due to friction, the sand at the interface will be dragged by the bag material as it moves. This will create a shear band close to the boundary. The sand outside this region will largely be unaffected, as shown by DeJong & Frost (2002) with compacted dyed and non-dyed sand particles sheared on a steel-alloy sleeve. The amount of particle interlock at the boundary is dependent upon the bag surface roughness, sand roughness, particle angularity and mean grain size of the sand.

The tension in the bag material will not be uniform across the bag given the interface is not frictionless, contrary to the Matsuoka & Liu (2003) model. As mentioned in the literature review, the earthbag is likely to fail at the top and bottom faces hence it can be assumed the bag reaches tensile capacity only at these points. This is assuming that the geometry of the bag is such that $H_0/B_0 \leq 1$, if $H_0/B_0 \rightarrow K_p$ then the tension in the bag material will be more uniform, thus the bag could fail at the sides.

4.2.1 Assuming earthbag cross section as rectangular

Considering particle interlock at the boundary interface, the horizontal boundaries can be considered similarly to a geogrid in a soil reinforced wall with the sides of the earthbag as rigid parallel vertical walls. This analogy will be used to analyse the compressive strength of an earthbag.

Assuming the volume of the earthbag does not change during compression the width of earthbag can be related to the amount of vertical displacement the earthbag experiences according to equation (4.2). It can be seen from the equation that when $x \rightarrow H_0$, $B \rightarrow \infty$.

$$V_0 = B_0 H_0 l = B H l. \quad (4.1)$$

$$B = \frac{B_0 H_0}{H_0 - x} \quad (4.2)$$

$$H = H_0 - x \quad (4.3)$$

The change in perimeter (ΔL) with respect to the initial perimeter (L_0) can be expressed in relation to the displacement of the platen as shown in equation (4.4) and by Tantonio (2007).

$$\frac{\Delta L}{L_0} = \frac{x(B_0 - H_0 + x)}{(H_0 - x)(B_0 + H_0)} \quad (4.4)$$

This can be used to express the tensile stress in the bag for a plane strain condition as shown in equation (4.5), where E is the stiffness of the bag material.

$$\sigma_{bag} = E \frac{\Delta L}{L_0} \quad (4.5)$$

$$\sigma_{bag}^{limit} t l = T_{limit} \quad (4.6)$$

Thus substituting equation (4.4) into (4.5) the quadratic can be solved to find the vertical displacement of the platen (x) at which the bag material reaches its tensile capacity:

$$x_{failure} = \frac{1}{2} \left[\left(H_0 - B_0 - \frac{\sigma_{bag}^{limit}}{E} (B_0 + H_0) \right) + \left(\sqrt{(H_0 - B_0)^2 + (H_0 + B_0)^2 \left(2 + \frac{\sigma_{bag}^{limit}}{E} \right) \frac{\sigma_{bag}^{limit}}{E}} \right) \right] \quad (4.7)$$

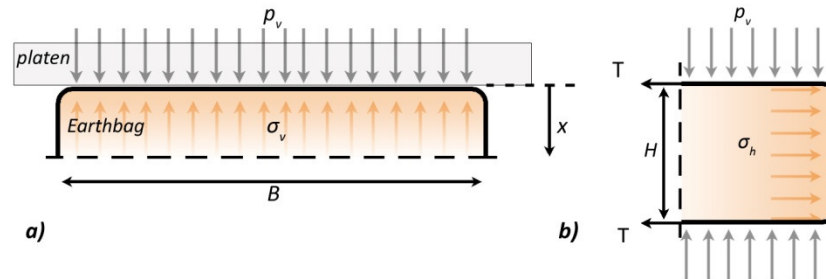


Figure 6: Free body diagram a) vertically and b) horizontally through earthbag under uniform vertical loading.

Taking a free body diagram vertically and horizontally through the earthbag and resolving forces results in:

$$\sigma_h = \frac{2T}{Hl} \quad (4.8)$$

$$\sigma_v = p_v \quad (4.9)$$

Where σ_h and σ_v are the vertical and horizontal stresses experienced by the soil and p_v is the external applied vertical stress. Thus the horizontal stress experience by the granular material is a function of the tension in the bag material. The vertical compressive stress is an unknown which must be defined to give the uniform vertical load an earthbag can withstand. The relationship between the vertical and horizontal stress experienced by the soil can be represented by the stress ratio K , which is a property of the material fill;

$$K = \frac{\sigma_v}{\sigma_h} \quad (4.10)$$

The stress ratio K is not constant because the behaviour of the granular material is inelastic and non linear, but for this model will be considered constant. The principal vertical and horizontal stresses can be represented on a Mohr-Coulomb diagram (see Figure 7), from which the stress ratio K can be found in relation to the friction angle of the fill (φ).

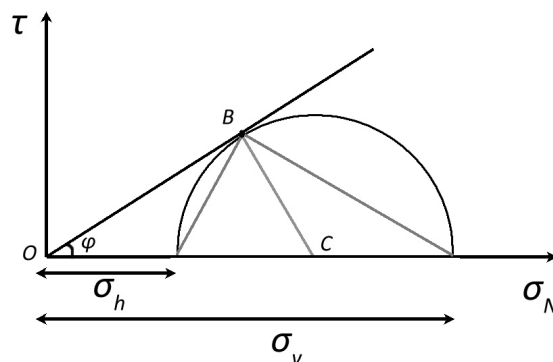


Figure 7: Mohr's Circle showing failure envelope of the earthbag where $\sigma_v > \sigma_h$.

From Figure 7:

$$\frac{\sigma_v - \sigma_h}{\sigma_v + \sigma_h} = \sin \varphi \quad (4.11)$$

$$\sigma_v = \sigma_h \frac{1 + \sin \varphi}{1 - \sin \varphi}$$

Where:

$$K_p = \frac{1 + \sin \varphi}{1 - \sin \varphi}$$

Hence it can be seen from equation (4.11) that an increase in the internal friction angle of the soil results in a lower horizontal stress for the same exerted vertical stress. Thus an increase in friction angle increases the overall stiffness of the earthbag and load carrying capacity. The relationship between horizontal stress and vertical stress is represented by equation (4.12) where it can be seen an increase in the ratio of B/H would improve the compressive strength of the earthbags as the horizontal stress would be lower for a particular load.

$$p_v = K_p \left(\frac{2T}{Hl} \right) \quad (4.12)$$

$$\therefore \text{At failure } p_v = \frac{2\sigma_{bag}^{limit} t}{H} K_p \quad (4.13)$$

Using equation (4.7) the displacement of the platen at which the bag ruptures can be found hence the value of H, from which the failure load $P_v^{failure}$ can be deduced from equation (4.14). The units for σ_{bag}^{limit} in equation (4.14) are N/mm², however, in §6.2 and §6.3.4 σ_{bag}^{limit} is taken as N/mm⁻¹ to avoid relying on the thickness (t) of the sample which can lead to inaccuracies, and thus t is taken out of the equation.

$$P_v^{failure} = p_v Bl = 2\sigma_{bag}^{limit} t l \frac{B}{H} K_p \quad (4.14)$$

4.2.2 Assuming earthbag cross section with semi-circular lateral edges

Another model which can be used is to consider the lateral edges as semi-circular as shown below and proposed by Tantonio (2007). In this model the stress ratio, K, is assumed to be equal to 1 at the edges, to create semi-circular boundary, and 3 in the middle of the earthbag. The initial perimeter and volume of the bag are defined in equations (4.15) and (4.16) respectfully. Again assuming the volume stays constant, the width of the bag can be found in relation to the position of the platen.

$$L_0 = 2B_0 + \pi H_0 \quad (4.15)$$

$$V_0 = B_0 H_0 l + \pi \left(\frac{H_0}{2} \right)^2 l = B H l + \pi \left(\frac{H}{2} \right)^2 l \quad (4.16)$$

$$\therefore B = \frac{4B_0 H_0 + 2x H_0 \pi - x^2 \pi}{4(H_0 - x)} \quad (4.17)$$

The perimeter of the bag after the bag has undergone deformation due to the loading platen is found by replacing equations (4.17) and (4.4) into equation (4.15) for B_0 and H_0 respectfully.

From this the change in perimeter with respect to the initial perimeter can be expressed which is used to find the tensile stress in the bag.

$$\frac{\Delta L}{L_0} = \frac{x(\pi x + 4B_0)}{2(H_0 - x)(2B_0 + \pi H_0)} \quad (4.18)$$

Substituting equation (4.20) into (4.5) we can solve the quadratic for the value of x at failure:

$$x_{failure} = \frac{1}{2\pi} \left[4 \left(B_0 + \frac{\sigma_{bag}^{limit}}{E} (B_0 + H_0\pi) \right) + \left(\sqrt{16B_0^2 + \left(4 \frac{\sigma_{bag}^{limit}}{E} \right) \left(8B_0^2 + 8B_0H_0\pi + 2H_0^2\pi^2 + \frac{\sigma_{bag}^{limit}}{E} (4B_0^2 + 4B_0H_0\pi + 2H_0^2\pi^2) \right)} \right) \right] \quad (4.19)$$

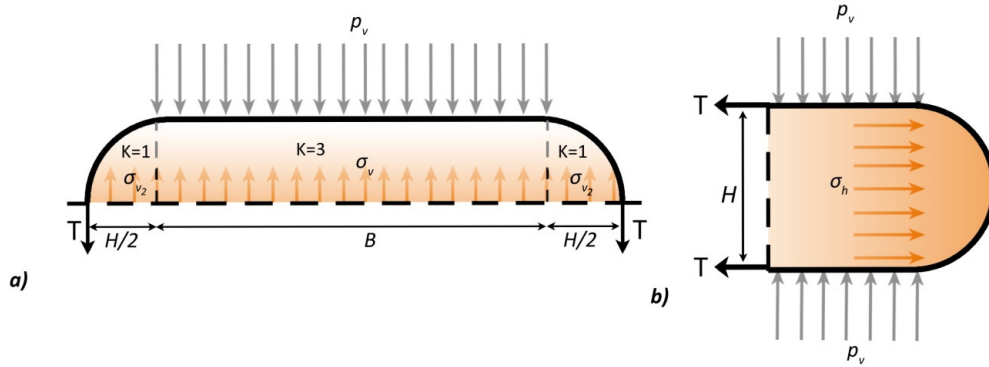


Figure 8: Free body diagram a) vertically and b) horizontally through earthbag with lateral semi-circular edges.

Taking a free body diagram vertically and horizontally through the bag the equilibrium of horizontal and vertical forces reads;

$$\sigma_h H l = 2\sigma_{bag} t l \quad (4.20)$$

$$\Rightarrow \sigma_h = \frac{2T}{H}$$

$$\sigma_v B l + 2\sigma_{v_2} \frac{H}{2} l = p_v B l + 2\sigma_{bag} t l \quad (4.21)$$

$$\Rightarrow \sigma_v + \sigma_{v_2} \frac{H}{B} = p_v + \frac{2T}{B}$$

Given the stress function is defined as $K=1$ at the edges $\sigma_{v_2} = \sigma_h$, thus substituting equation (4.20) into (4.21):

$$\sigma_v = p_v \quad (4.22)$$

The vertical applied stress can be expressed in terms of the dimensions of the bag as outlined by Tantonio (2007):

$$p_v = K_p \sigma_h \quad (4.23)$$

$$\begin{aligned} \therefore p_v &= K_p \frac{2\sigma_{bag}^{limit} t}{H} \\ \therefore p_v &= \left(\frac{1 + \sin \varphi}{1 - \sin \varphi} \right) \frac{Et x (\pi x + 4B_0)}{(H_0 - x)^2 (2B_0 + \pi H_0)} \end{aligned}$$

4.2.3 Summary of theoretical compressive strength of earthbag

It can be concluded from the two models that for a vertically loaded earthbag the compressive strength of an earthbag is dependent upon the tensile strength of the bag material and the friction angle of the soil, for the assumptions outlined in §4.1. The overall stiffness of an earthbag is more complicated, and is dependent upon several factors such as the stiffness of the bag material, compressibility of the soil and how the earthbags are restrained top and bottom.

Stabilising the soil will provide an initial cohesion which is represented by a vertical shift in failure line on the Mohr's circle which indicates that a higher vertical pressure is needed to cause failure of the earthbag. A similar affect can be seen with the introduction of clay to act as a binder and provide some cohesion to the soil. The corresponding relationship between vertical and horizontal pressure in the earthbag, assuming a rectangular section, is therefore:

$$\sigma_v = 2c' \sqrt{K_p} + \sigma_h K_p \quad (4.24)$$

$$\therefore \sigma_v = 2c' \sqrt{K_p} + \frac{2\sigma_{bag}^{limit} t}{H} K_p \quad (4.25)$$

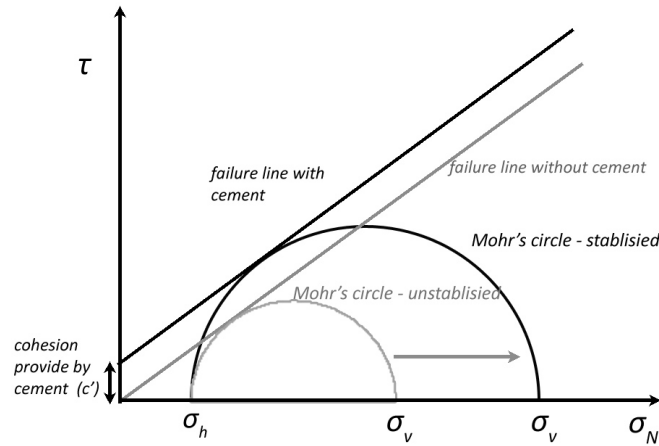


Figure 9: Mohr's circle showing the affect of the application of cement on granular fill.

It is expected that the relationship between stress and strain for the earthbag will be non linear. As the earthbag is compressed, lateral confinement of the soil is provided by the bag material; as previously shown the confinement force (T) increases with an increase in horizontal force applied by the soil, up to rupture. Thus, the stiffness of the earthbag is expected to increase as vertical applied stress increases. Hence it is important to initially compact the earthbag in construction as this improves the initial stiffness of the earthbag and reduces overall short term

deformation of the structure. Finally, a global shear band may develop when the stack height is sufficiently high such that end restraint effects are minor, as reported by Lohani *et al.*, (2006). The angle of the shear band can be found from plotting the experimental data on a Mohr's circle.

Although it is important to gain an understanding of the mechanics of earthbags under uniform vertical load; the vertical loads which an earthbag has to resist, in an earthbag house, are unlikely to reach the vertical load capacity of the earthbag.

4.3 Shear Strength of Earthbags

To predict a potential failure mode of an earthbag structure an understanding of how earthbags behave under direct shear is needed. From laboratory tests an experimental value for the coefficient of friction μ ($= \tan\phi'$) can be deduced. Furthermore the experiments will indicate potential improvements which could be made in construction and/or in material choices, which would improve the shear resistance of earthbag structures.

The shear between two earthbags can be described using a Coulomb friction model as defined in equation (4.26).

$$F_f = \mu F_N \quad (4.26)$$

From Coulomb friction analysis, it should be noted that the contact area between two bodies is proportional to the normal force applied; furthermore the frictional force is proportional to the applied normal force as defined by equation (4.26). For low applied normal forces the interaction between the two bodies becomes difficult to predict.

From the direct shear test between earthbags a value for μ is obtained for a particular material interface. It is predicted that the hessian bags will provide the greatest frictional interface. The barbwire will improve the shear resistance and provide an initial cohesion between the bags. The predominant mode of interaction between the barbwire and sand is likely to be bearing; with the points of the barbwire acting as dowels between the bags. Theoretically the mechanics of barbwire can be considered to be acting in a similar manner to a short pile undergoing lateral loading, as outlined by Broms (1964). If the earthbag is subject to direct shear the barbwire acts to resist the bag material moving and hence shear displacement of the earthbag as a whole. Failure of the earthbag in shear will occur when the bag material begins to tear as it tries to move past the barbwire point.

Figure 10 shows the theoretical modes of failures of the barbwire points under direct shear; beneficial shear force resistance in the barbwire point is considered negligible. The barbwire point is more likely to fail as a rigid body given the rotational resistance of the connection between the points is less than the bending strength of the barbwire material.

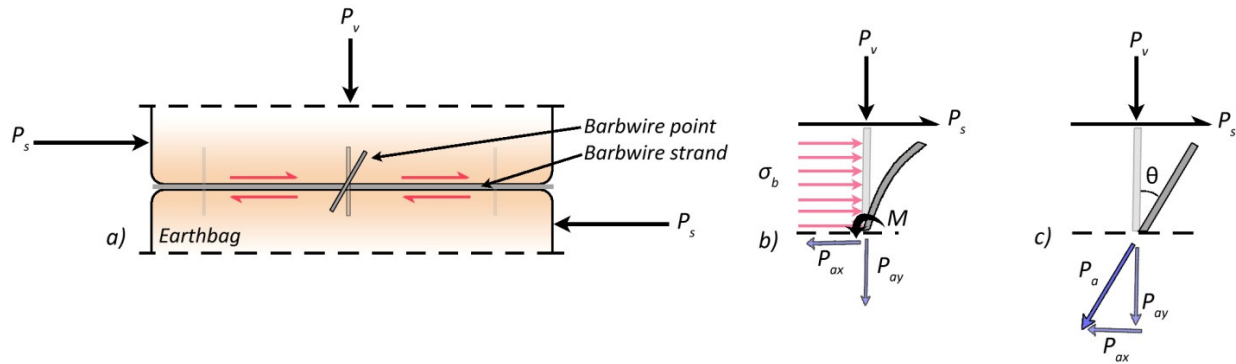


Figure 10: Theoretical failure mode of barbwire under direct shear a) overall view b) failure by bending c) rigid body shear failure.

Equilibrium of the soil about the rigid body is illustrated in Figure 11 showing lateral resistance is provided by passive earth pressure; note here the stress ratio is defined as $K = \sigma_h/\sigma_v$.

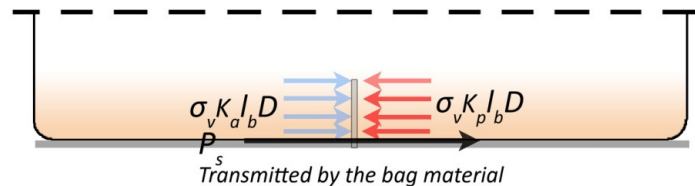


Figure 11: Force equilibrium about barbwire point showing lateral resistance of soil against applied lateral force from the soil and bag material.

From Figure 11 it can be seen that the lateral resistance of a barbwire point in a cohesionless soil and the applied lateral force on the barbwire can simply be expressed by equations (4.27) and (4.28) respectfully. The coefficient of friction between the soil and the barbwire is conservatively taken as 1. The barbwire point has some inherent initial resistance against lateral movement, which has been denoted by P_{ax} .

$$P_u = K_p \sigma_v D l_b + P_{ax} \quad (4.27)$$

$$P_l = K_a \sigma_v l_b D + P_s \quad (4.28)$$

4.4 Theoretical Earthbag Arch Mechanism

Traditional plastic analysis of masonry arch structures is considered to describe the theoretical behaviour of earthbag arches. As outlined by Heyman (1995), with plastic analysis the concern is with the ultimate limit state of the structure hence it is not concerned with the actual state of the structure, for which there is an infinite potential number of equilibrium conditions for the structure. Therefore this approach reduces the number of material properties that need to be defined given the structure is only considered in relation to ultimate state.

However, there are several differences which reduce the accuracy of the initial assumptions made for the plastic analysis of arch structures. Firstly it is assumed that sliding failure does not occur; however, the accuracy of this for an earthbag structure is dependent upon the friction coefficient between the bags and the compressive stresses normal to the interface. With the addition of barbwire between the earthbags it is expected the arch will be able to sustain much greater deformations before collapse. Furthermore the contact area between the bags is likely to vary less throughout loading, in comparison to arch tests without barbwire, as the barbwire acts to grip the bags together. Analysis has been undertaken, (e.g. Livesley, 1978; Gilbert *et al.*, 2006) to consider potential rotations, separation and sliding of masonry blocks in computational analysis to provide a more accurate model of the behaviour of masonry arches, but is outside the scope of this dissertation.

It is also assumed that the material has infinite compressive strength. Given the applied loads relative to the compressive strength of the earthbags is safe to assume that the structure will not fail due to crushing of the bags. However, local deformation is likely to occur, which would alter the component section profile and thus the behaviour of the structure in relation to the applied load. The level of local deformation is dependent upon the material fill (including any stabilisation), bag material stiffness and initial compacted state of the earthbag. Thus for a stabilised earthbag filled with dense coarse sand, the behaviour under a point load will be similar to that of a masonry arch. Finally it can be assumed that the earthbag is incapable of carrying tension, which is safe to consider.

Considering the case where the thrust transmitted between earthbags reaches the extrados of the arch, the assumption of no tension capacity becomes significant. As the thrust line reaches the surface, rotation of the earthbag occurs creating a hinge at this point. The hinge signifies the point at which the load has reached the edge of the arch, any further movement of the thrust line would mean the thrust line is outside the section area of the arch and thus failure of the arch occurs. In addition no further moment can be sustained at this hinge location, if additional load is applied however, hinges can occur elsewhere in the arch given there is still redundancy. Thus the formation of a hinge has generated a redistribution of bending moments in the structure, allowing the structure to carry a greater load after the initial hinge. Failure of the arch only occurs when sufficient hinges have formed to transform the stable arch structure into a mechanism which is statically determinate. For a point load at quarter span on an arch, the failure load will be the load at which four hinges are formed along the line of thrust as shown in Figure 31. Using computer software an iterative approach can be used to find the thrust line, hence hinge locations which will yield the minimum collapse load of the structure.

5 Laboratory Testing

5.1 Soil Analysis

5.1.1 Sieve Test

A dry sieve analysis was performed in accordance to BS 1377-2:1990 Clause 9.3, with altered sieve sizes as shown in Appendix A. A fine builders' sand was used to best replicate the sand found in the Namib Desert.

5.1.2 Shear Box Tests

Shear box tests were carried out in accordance to BS 1377-7:1990 to find the internal friction angle of the sand and shear strength of the sand. Sand samples were compacted by different amounts and categorised as either very dense, medium dense or loose. The same sand was used for all the experiments undertaken in this dissertation however the moisture content varied between tests. The dimensions of the shear box were 100mm x 100mm x 50mm, however sample depths were taken lower than 50mm to allow full fit of the loading cap. Shear displacement was set at 1mm/min and normal loads of 0.314kN 0.804kN and 1.295kN were applied.

5.2 Tensile Tests on Bag Material

Tensile tests were carried out on 70gsm polypropylene (good and poor condition), 100gsm polypropylene and hessian bags using a constant rate of extension machine (DARTEC 20T machine). 70gsm polypropylene bags were taken from the prototype build by FCBS, which had been exposed externally for 172days being subject to UV, rain and snow during this period. Samples were cut at least 150mm from the edge of the bag to 30mm x 200mm width and length, respectively. Due to the limitations of laboratory equipment at the University of Bath, a wide strip method is not viable. Balsa wood pieces were put between the grips to ensure the specimens did not fail at the ends from the friction between the grips. The interface between the balsa and the bag material was marked so any slipping of the material could be identified. No pretension was applied to the specimens. Extension rate was initially set at 5mm/min.

5.3 Compression Tests

The aim of the compression tests was to gain an understanding of the behaviour of earthbags under vertical load and quantify the compressive strength of earthbags with variation in bag material and material content. To achieve this several compression test using a DARTEC 200T machine were performed as outlined below;

- Single 20kg hessian, 70gsm and 100gsm polypropylene bags
- 3 bag stack – 10/15/20kg, 100gsm polypropylene bag
- 8 bag stack – 20kg 100gsm polypropylene bag
- 8 bag stack – 20kg 70gsm polypropylene bag

- 8 bag stack – 20kg stabilised 100gsm polypropylene bag

Dry sand was used to fill the bags. The earthbags were then ‘diddled’, a process whereby the corners of the bag are pushed inward to ensure they do not expand out during the compression test. Compaction of the bags using a 12.6kg tamper occurred on the loading platform to ensure the specimen was fully compacted before loading. Dimensions of the bag were recorded and the bag was levelled to ensure the stack did not undergo rotation. 30mm thick steel plates were positioned top and bottom of the earthbag stack to ensure a uniform compression was applied to the bags. Compressive tests with 3 and 5 bags had two strands of 3 point barbwire between the bags to replicate the actual construction case. However, for the 8 bag stack barbwire was not used due to concerns of barbwire resisting lateral spreading of bag material. Load was applied such to maintain a constant displacement of 10mm/min. For the 1, 3 and 5 bag stacks, the specimens were taken past failure point to gain an understanding of the behaviour of earthbags beyond initial tearing of the bag material. Testing was stopped for the 8 bag stack soon after the sample had a loss in load carrying capacity.

For the 8 bag stack tests transducers were used to measure the deformation of the bags. Transducers were positioned at the long side of the bag to measure the level of lateral expansion and at the short side of the earthbag to verify the assumption of plane strain; Figure 12 and Figure 20 show the location of the transducers. Transducers were not positioned on both sides of an earthbag as it is thought the expansion of the earthbag would be fairly symmetrical either side. The deformation of the bags may vary throughout the stack with the earthbags furthest from the support being less subjected to end restraint effects hence can expand more freely. To verify this assumption, transducers recorded movement of an earthbag in the middle of the stack and one near the restraint. Profiles of the earthbag edges were replicated using a profile gauge which was used to mark out the profile onto wood pieces. The wood pieces were then attached at transducer locations using car body filler.



Figure 12: Arrangement for eight earthbag stack compression tests

It must be noted that the steel plates became significantly bent through compression of the earthbags during the 1, 3 and 5 earthbag(s) stack tests hence the contact area between the platen and earthbags was not uniform. To avoid this problem occurring again for the 8 bag stack test, the lower jaws of the machine was removed and the earthbags were loaded onto the steel base of the machine.

For the stabilised case 4% general purpose cement was added to the sand with a moisture content of 6.5% and left to cure for 36 days. Unfortunately the bags were left longer to cure than those used for the arch test (7 days), due to availability of machinery, so the measured compressive strength of the earthbags will be higher.

5.4 Shear Tests

Earthbags were sheared in a large scale direct shear box apparatus (see Figure 13) with a specimen size of 300 x 253 x 110mm. A large scale shear box was used as it provided lateral confinement to the bags, hence the contact area between bags stayed constant throughout testing. Although the coefficient of friction is independent of the contact area, to obtain a magnitude of shear stress resistance between the bags to use for analysis a contact area size must be known. Furthermore the frame ensured the applied shear force was uniformly applied to the earthbag. The internal dimensions of the shear box are 300 x 300 x 100mm (200mm for both boxes). A similar testing procedure as outlined by BS 133-7:1990 was performed. A list of the direct shear tests performed is given below;

- 100gsm Polypropylene - Normal loads 2.2 / 7.1 / 12.0 / 16.9kN without barbwire.
- 100gsm Polypropylene - Normal loads 2.2 / 7.1 / 12.0kN with barbwire
- Hessian – Normal loads 2.2 / 7.1 / 12.0kN without barbwire

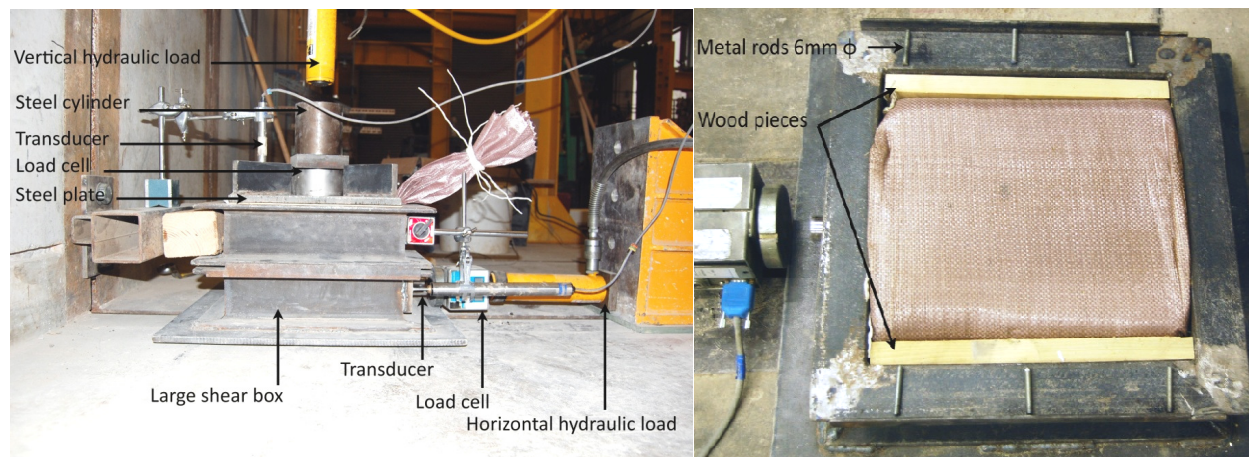


Figure 13: Earthbag shear test apparatus

Steel rods were placed underneath the shear box as bearings. Polypropylene 100gsm bags were filled with 13kg of sand and compacted within the shear box. The width of the earthbags were smaller than width of the shear box, hence to provide lateral confinement two wood block were placed either side of the bag.

At the sides of the steel frames the Teflon strips were replaced with small steel rods to raise the steel frame boxes and ensure the only contact areas between the boxes was between the bags (see Figure 13). To check the friction of apparatus, a test with just the apparatus and no normal load was done. Negligible horizontal load was required to move the bottom steel frame.

For the tests with barbwire, two strands of 3 point barbwire were placed between the bags. The horizontal load was applied and the vertical load was maintained using a hand operated hydraulic jack system. For the earthbag without barbwire and hessian tests the bags were not replaced between load experiments. For the tests with barbwire, the bags were checked after each test for damage, if substantial damage had been sustained by the bags then they were replaced. Transducers were used to measure horizontal displacement of the bottom steel frame and vertical displacement of the top steel plate. Applied load and displacements were logged using a computer.

5.5 Arch Test

The arch test provides an insight into how the earthbags work as a structure and potential modes of failure it may have. Furthermore the experiment will give a better understanding on the effect of material factors on the failure mode of the arch. Of particular concern with earthbag structures is the level of deformation under loading, thus, a stabilised arch is considered to quantify the improvement in stiffness with the addition of cement. A full size dome could not be built due to the limitations in laboratory space, time and resources. Furthermore obtaining accurate data from the dome would be complicated. A scale model of a dome was considered using lead shots to represent sand grains given they would have a similar friction angle, however, scaling the barbwire and bag material proved problematic. The following experiments were undertaken (all with 100gsm polypropylene bags);

- Point load at quarter span – unstabilised bags, no barbwire between bags (x2)
- Point load at midspan - unstabilised bags, no barbwire
- Point load at quarter span – stabilised bags, no barbwire
- Point load at quarter span – unstabilised bags, with barbwire

Earthbags were placed to form an arch between two concrete roller abutments and loaded by a point load either at quarter span or mid span. The connection between the arch and abutment is considered to be fixed. The abutments were tied together by rebar with a load cell between either set of rebar to measure horizontal reaction force at the abutments. The rise and span of the arch was 1:4.10, respectively. Formwork was placed on jacks such to allow it to be lowered and removed once the earthbags had formed an arch. The earthbags were compacted on the ground then lifted into place and further compacted using a wood piece and mallet. This process was found to provide a more uniform compaction than tamping the bags on the formwork, which became increasingly difficult towards the keystone. Producing bags of uniform thickness was difficult thus leading to an inconsistent number of bags used per arch test. The bag thickness can be moderated if the length of the bag during compaction is strictly controlled.

Formation of the keystone required two earthbags with reduced fill and compaction so that they formed a wedge shape. Once in place the keystone was compacted from above to ensure full bearing onto neighbouring bags. For the barbwire arch, inserting the keystone in the same way would result in tearing of the bags. To avoid this, two metal sheets were positioned on the faces

of the neighbouring bags to the keystone (protecting the keystone from the barbwire). The keystone was then inserted and the sheets were removed, finally the keystone was compacted from above as before.

LVDT transducers were positioned at quarter spans and mid span. In addition a camera was set up on a tripod and the face of the bags was marked to record movement of the arch. The camera we set up in the same location for all arch tests. A point load was applied using a hydraulic jack onto a roller and steel plate with a wood piece underneath to spread the load across one bag to prevent significant localised deformation (see Figure 14). To ensure a uniform contact area between the wood piece and earthbag dental paste was applied between the wood and earthbags. Deflections of the arch at quarter spans and mid span were measured during formwork removal. Furthermore the horizontal distance from the centre of the arch to the wall was measured before and after formwork removal, such that any out of plane rotation of the arch could be detected.

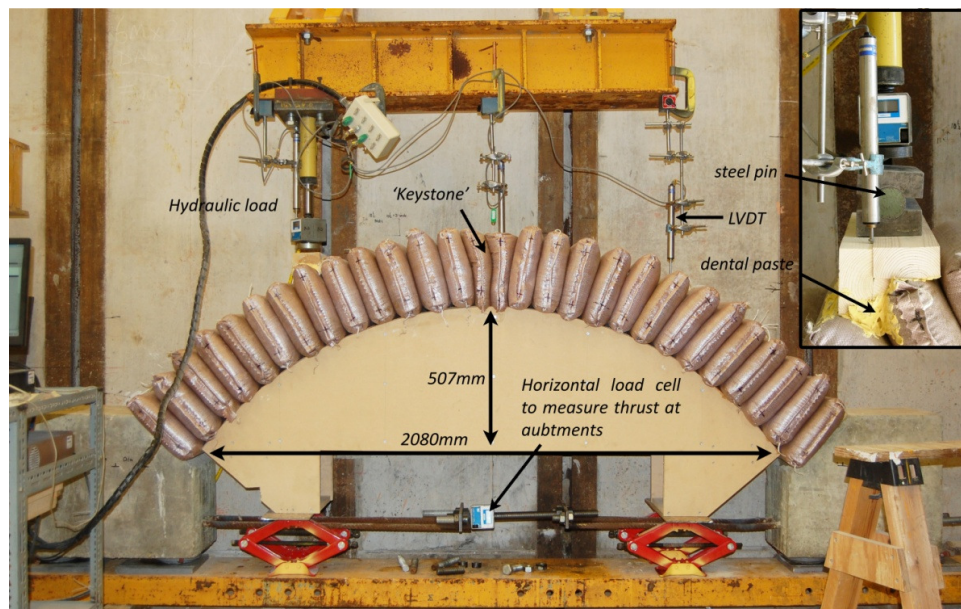


Figure 14: Arch test apparatus

5.5.1 Stabilised Arch Tests

A similar procedure was used for the stabilised arch tests as the unstabilised, except, 4% (8kg) general cement was added to the sand. The sand was sufficiently damp, with a moisture content of 6% so no water was added. The earthbags were compacted and placed on the formwork and allowed to cure for 7 days before being tested.

6 Results & Analysis

6.1 Soil Analysis

6.1.1 Sieve Tests

The results of the sieve tests are shown in Figure 33 and Figure 34, Appendix A. Comparing the results with the dry sieve analysis from Namibia, it can be seen that the two samples are similar as the majority of sand particles are fine – medium. The sand from Bath is finer with the 66% of the sand being retained by the 125 μ m sieve, whereas the sand Namibia had 63% retained by the 250 μ m sieve.

6.1.2 Shear Box Tests

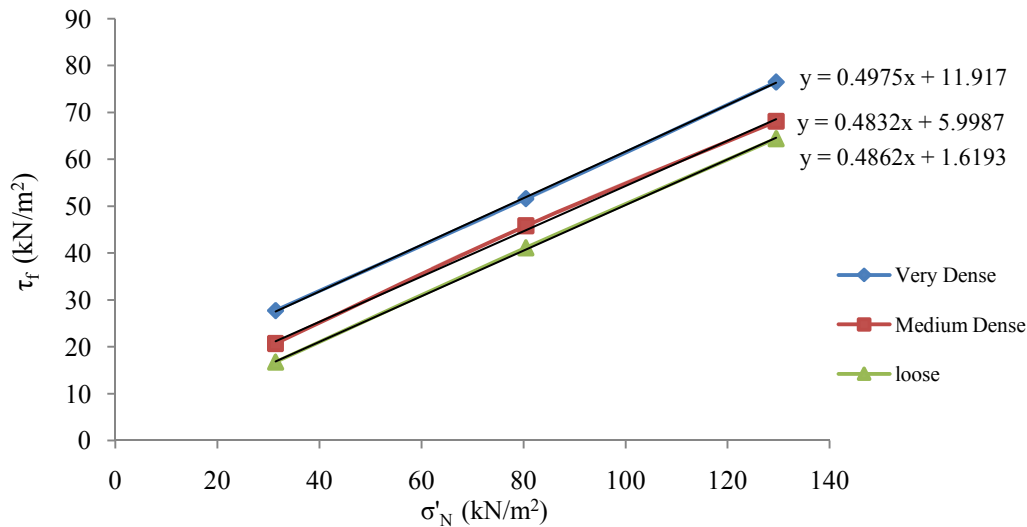


Figure 15: Shear box test; shear stress at failure against effective stress normal to the failure plane.

The corresponding densities for the tests were 16kN/m³, 15.5kN/m³ and 13.88kN/m³ for the dense, medium dense and loose samples, respectively. From Figure 15 the internal friction angle of the sand sample can be found as outlined below;

$$\text{For a granular material:} \quad \tau_f = \sigma'_N \tan \varphi' \quad (6.1)$$

$$\begin{aligned} \text{Very Dense sample: } 0.498 &= \tan \varphi' \quad \therefore \varphi' = 26.5^\circ \\ \text{Medium Dense sample: } 0.482 &= \tan \varphi' \quad \therefore \varphi' = 25.7^\circ \\ \text{Loose sample: } 0.486 &= \tan \varphi' \quad \therefore \varphi' = 25.9^\circ \end{aligned} \quad (6.2)$$

The initial density of the sand does affect the internal friction angle of the sand, given a greater shear force is required to overcome particle interlock in addition to the force required to overcome interparticle friction. Hence, for use in calculating value of K_p for the earthbag

compression test, the initial earthbag density was recorded. The density of the sand used in the earthbag compression tests is given in Appendix B (see accompanying C.D).

6.2 Tensile Test on Bag Material

Table 1 shows the maximum tensile strength of each sample performed in the tensile tests. Figure 16 is the stress strain relationship for each sample;

Table 1: Tensile strengths of all bag material samples obtained from tensile tests.

Material	Exposed length (mm)	Initial width (mm)	Strain at tensile limit (%)	Tensile stress (N/mm per mm thickness of material)	Young's Modulus E (N/mm per mm thickness of material)
Polypropylene 100gsm (1) -	100	30	16.2	20.9	129.5
Polypropylene 100gsm (2)	137	30	14.5	18.6	128.6
Polypropylene 100gsm (3)	135	30	13.9	15.3	109.8
Polypropylene 100gsm (4)	185	30	14.5	18.2	125.6
<i>Average (sample (3) disregarded)</i>			15.1	19.2	127.9
Polypropylene 70gsm (good condition)	100	30	17.1	9.7	56.6
Polypropylene 70gsm (poor condition)	137	30	14.2	8.3	58.6
Hessian	100	30	2.7	8.9	324.9

All polypropylene 100gsm had a thickness of 0.17mm

12/3/10

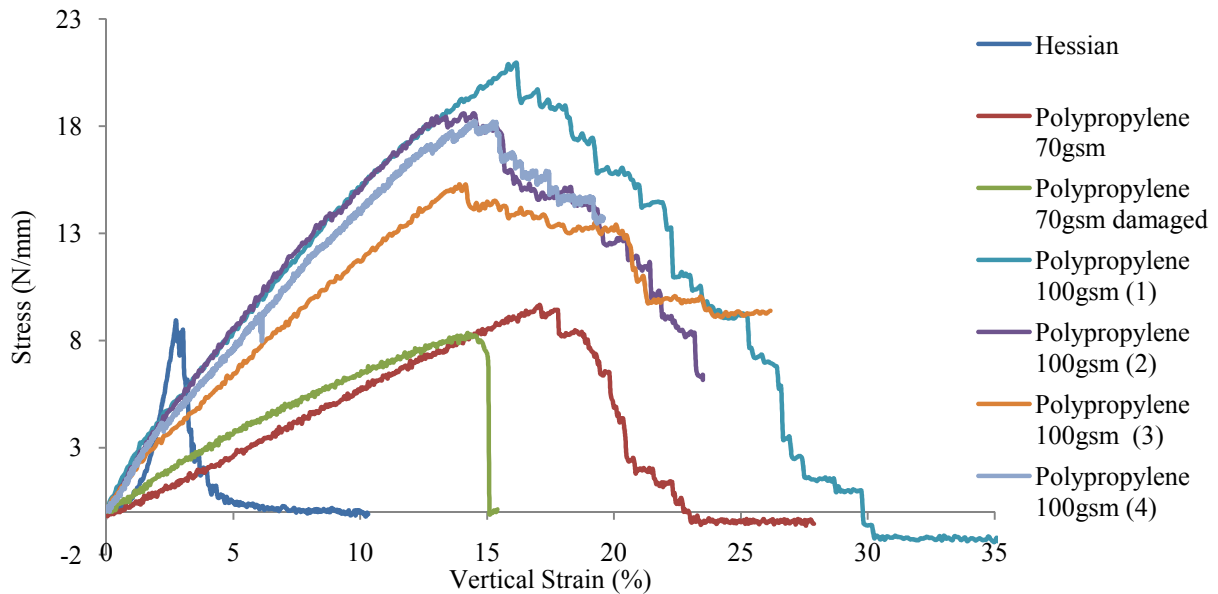


Figure 16: Stress strain relationship from tensile tests of all bag material samples.

Note, measured stress and stiffness of the samples are per unit thickness of the bag material to avoid errors due to inaccuracies in measurements of bag thickness. From the experiment it is clear that the 100gsm polypropylene bags have the highest tensile strength and have around double the stiffness of the 70gsm polypropylene used by FCBS, under uniaxial tension. The damaged 70gsm polypropylene sample did not experience a large reduction in tensile strength but was subject to brittle failure. Hence indicating that if an earthbag structure, made with polypropylene bags, is left unprotected (i.e. no render is applied) then the earthbags are subject to abrupt rupture if the tensile stresses in the polypropylene reaches the tensile capacity of the polypropylene. However, a high vertical force is still required to cause rupture of the bag material which is unlikely to be reached during the earthbags lifespan; i.e. assuming bag dimensions at failure of $235 \times 452.5 \times 105 \text{mm}$ ($B \times l \times H$), $K_p = 2.6$ and $\sigma_{bag}^{limit} = 8.3 \text{N/mm}$ and using equation (4.14) $P_v^{failure} = 43.7 \text{kN}$.

The sample width was assumed to be constant until the point at which maximum tensile stress was reached in the material. However, this was not always true as some samples experienced slight necking before capacity was reached. Furthermore, obtaining useable samples from the hessian bags proved difficult as cutting the hessian left frayed edges, which would have affected the load carrying capacity of the strip. Thus the accuracy of the experiment would have increased if a wide strip was used.

6.3 Compression Tests

Compressions tests on earthbags were performed as outlined in §5.3 to gain an understanding how the earthbags behave under vertical loading, some of the results are outlined below. Compression tests were performed on single bags, however, the tensile capacity of the polypropylene bag was never reached owing to end restraint effects. Thus the data is not a true representation of the earthbag capacity and will not be considered further.

6.3.1 Three earthbag stack

The force displacement relationship will be considered first given no theoretical assumptions are needed to create this graph, thus can be considered reliable. Figure 17 shows the earthbag's behaviour under uniform vertical loading was non linear. It is believed at the point prior to strain softening the polypropylene had reached tensile capacity; hence it is this region which is of primary concern for the design of earthbag structures and is taken as the failure point of an earthbag under vertical loading. Tearing at the sides of bag was not seen during this period; however, cracking was heard indicating tearing. Tearing on the top faces was noticed at the end of the test when the steel plates were removed.

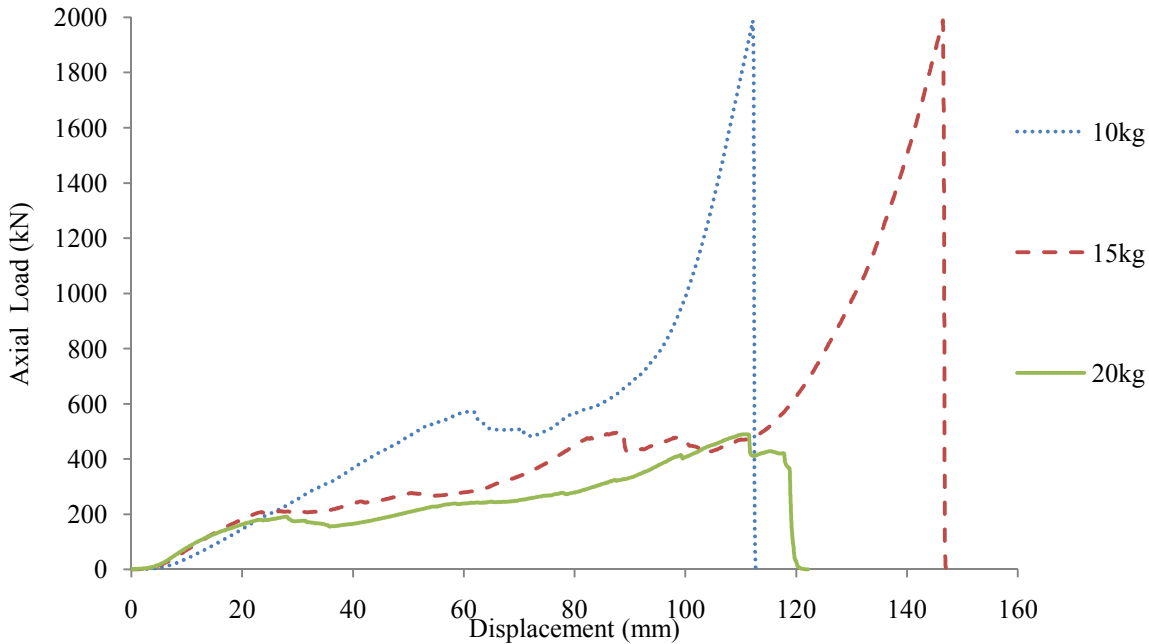


Figure 17: Compression test results of three 100gsm polypropylene earthbags with varying amount of fill.

Frictional forces generated at the plate interface and the barbwire between earthbags would, to some extent, resist extension of the bag material thus increase the load required to cause tearing. Conversely, the barbwire created holes in the bag material, therefore as the bag attempts to expand laterally under uniform vertical load there would be a higher stress concentration around the holes. This would have somewhat increased the rate at which tearing of the bag material occurs. A similar effect is seen between the plate and earthbag due to the rough surface of the steel plate resisting movement of the bag material.

After the tensile capacity of the bag material had been reached, the stiffness of the earthbag reduced for 15kg and 20kg earthbags. Although the bag material had reached its tensile capacity, the earthbag is still able to sustain an overall positive load displacement relationship. It is believed that frictional forces generated between the polypropylene and sand resist translations of the sand particles at the top and bottom faces, as discussed in §4.2. As the pressure increases, the sand confinement in the region underneath the applied load increases i.e. the void ratio reduces. Thus there is a highly dense region of sand through the centre of the bag, with more dilated edges, such that a high proportion of the load is transferred through the central portion of the earthbag. Consequently subsequent tearing of bag material does not yield complete collapse of the earthbag as the sand is less reliant on the confinement provided by the polypropylene. Eventually an increase in shear stresses acting on the top and bottom faces of the earthbag causes rupture of the sand block, which is represented by a sharp fall in the force displacement graph. The bag material prevents sand from escaping the bag, thus the earthbag can still carry load.

Subsequently for the 15kg earthbag there was a rapid increase in load carrying capacity. It is thought that as the sand becomes more confined the stiffness of the sand region under vertical loading increases, hence the level of particle interlock rises. Thus, for failure to occur high shear stresses are required not only to overcome frictional resistance but also particle interlock. Vertical dilatancy is prevented by the high vertical applied stresses thus yielding an exponential load displacement relationship. Furthermore the ratio of height to width of the bags is greatly reduced at this point, thus the end restraint effects become hugely significant as with the single bag compression tests.

It is not imperative that a defined conclusion on the behaviour of earthbags under such loading is made given these loads will never be experienced by earthbag structure. Of primary concern for the design of earthbag structures is their behaviour under working loads, well below the load at which the tensile strength of the bag is reached. Figure 18 shows an enlarged section from the load against normalised vertical displacement graph. Initially all three graphs have a low resistance against vertical displacement, given some particles are still in a loose state and can collapse into the surrounding voids. After which the sand moves laterally, initiating the bag material into tension, such that the subsequent load displacement relationship is largely dependent on the stiffness of the bag material. The 20kg bags had the lowest load capacity as overall the stack height was greater thus the end restraint effects were less.

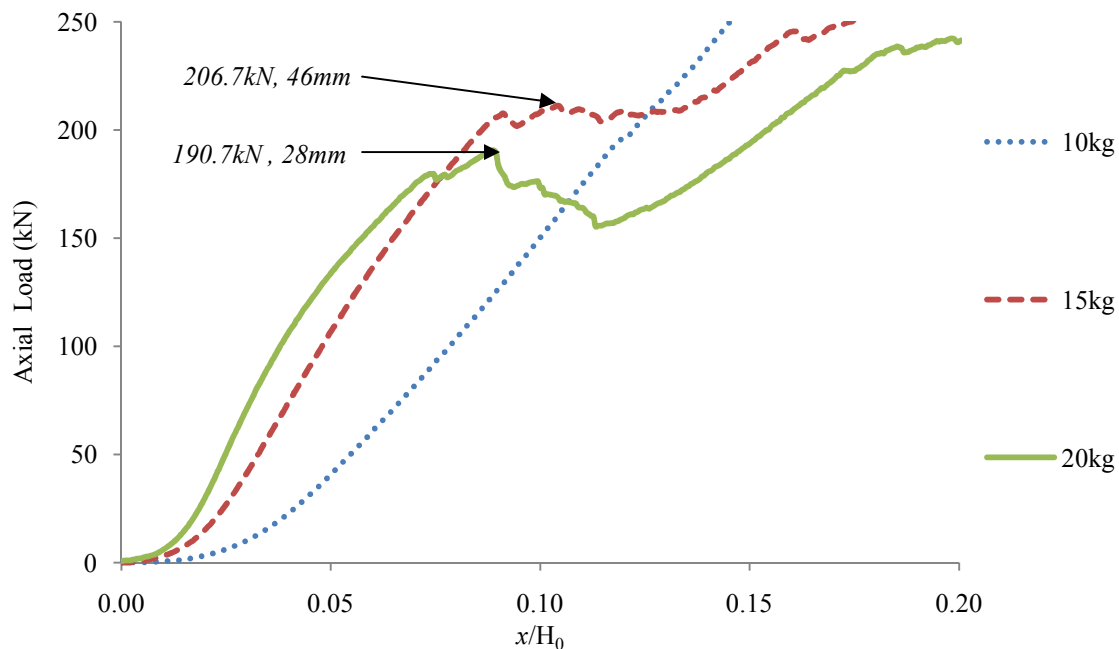


Figure 18: Three earthbag 100gsm polypropylene stack compression test showing enlarged section of load displacement graph.

6.3.2 Five earthbag stack

The 5 bag stack was less susceptible to end restraint effects than the 3 bag stack, therefore failed at a lower vertical stress. Cracking of bag material fibres was heard around 135kN. The stack did display some buckling during testing however the bag underwent local deformations which meant the stack remained stable. The ratio of H_0/B_0 , where H_0 is the total initial height of the stack, for the five bag stack was measured to be 2.2. In comparison to the eight bag stack, this is not sufficient to remove significant end restraint effects. Thus, a value of $H_0/B_0 \geq 3.0$ should be taken. This may vary between different bag materials given the 70gsm polypropylene earthbag test had a $H_0/B_0 = 2.5$ and did not demonstrate any inaccuracies due to end restraints. In Figure 19 the calculation of stress and $\Delta L/L_0$ uses theoretical widths as calculated from equation (4.2).

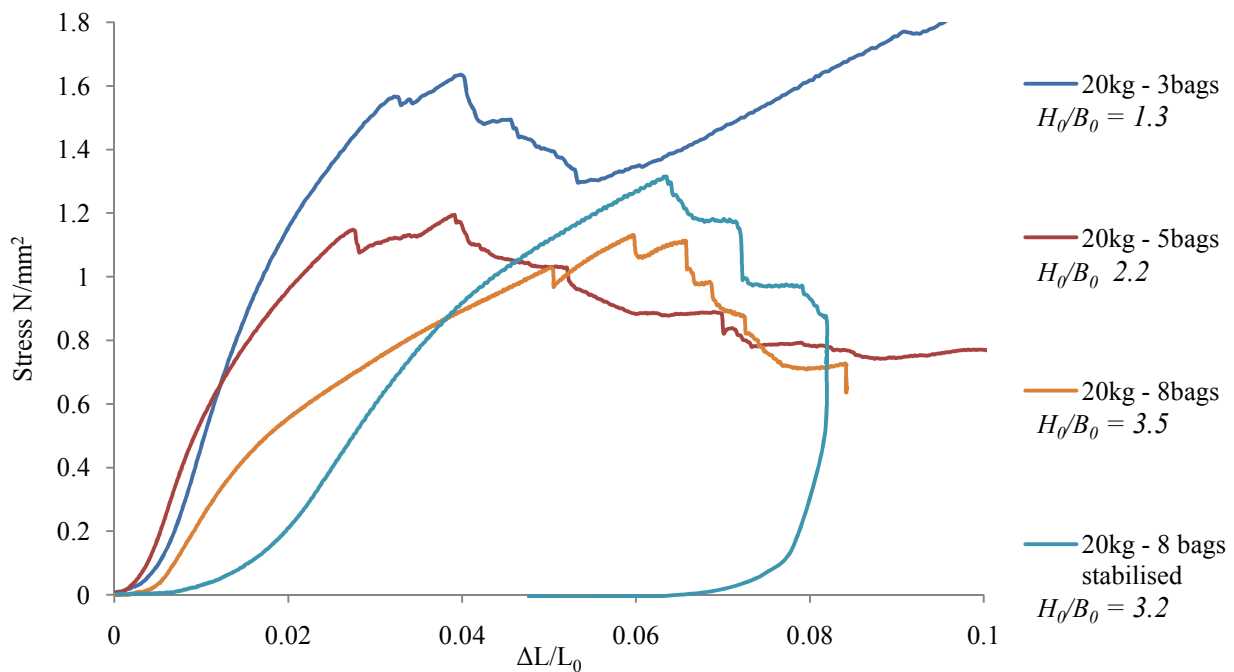


Figure 19: Stress strain relationship of earthbags in compression, with variation in stack height

6.3.3 Eight earthbag stack

An altered experimental procedure was used for these tests, given the used of transducer as discuss in §5.3. Figure 20 indicates the location of the transducer along the 8 bag stack.

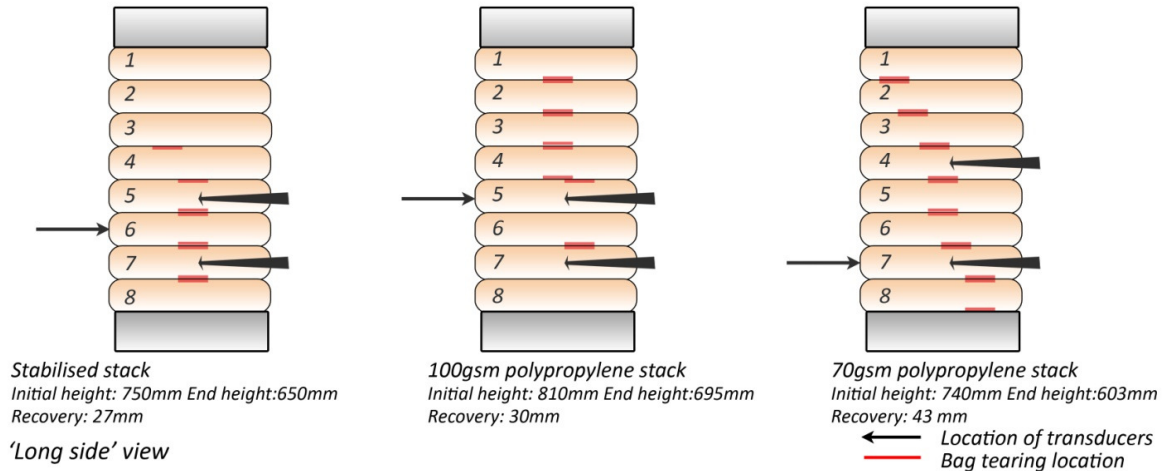


Figure 20: Location of transducers, failure points in bag material and recover of earthbag stack after unloading

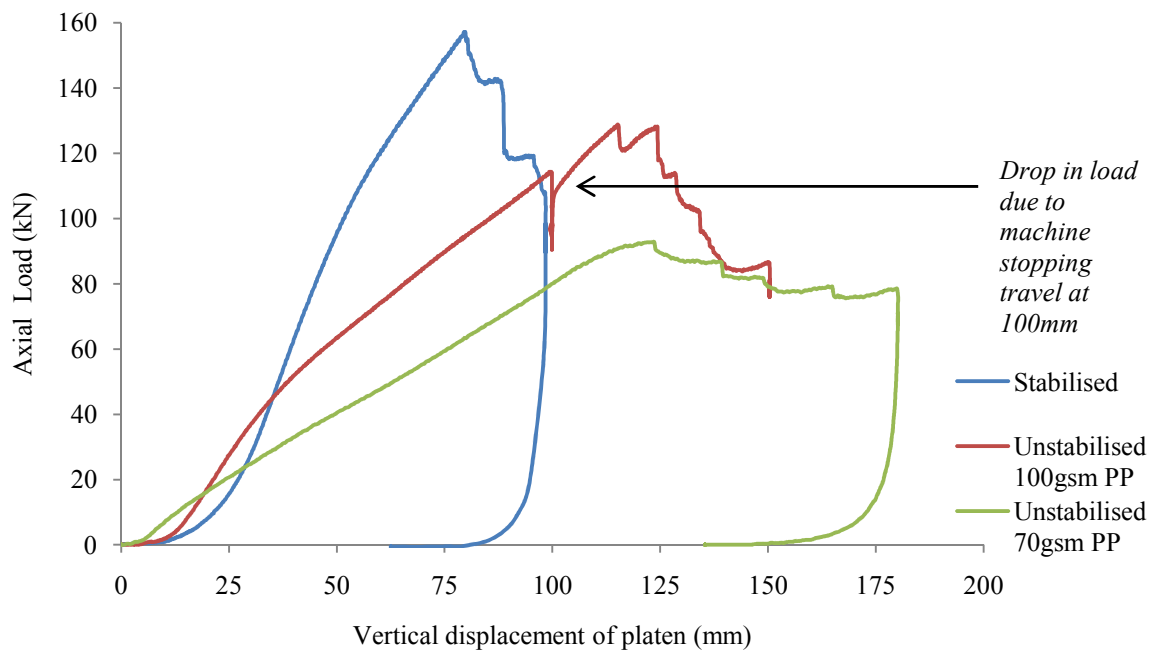


Figure 21: Load displacement graph for eight stabilised 100gsm polypropylene, unstabilised 100gsm polypropylene and unstabilised 70gsm polypropylene earthbags.

6.3.3.1 Unstabilised 100gsm polypropylene earthbag

As before, the behaviour of the earthbags underwent an initial rapid rise in stiffness. In relation to previous experiments, the behaviour then onwards till failure is much more linear. Given there is less restriction against movement of the bag, the bag material is fully initiated in tension therefore this linear behaviour corresponds to the extension of the bag material. Cracking was heard around 120kN (1.10N/mm^2) relating to tearing of the bag material. Unlike the five earthbag stack, buckling of the stack was not experienced. Accurate measurements of bag dimensions using the transducers become difficult towards the end of the test. At 100mm vertical

displacement, the transducer measuring expansion on the short side of the bag was at the edge of wood piece. There was also noticeable rotation of the wood pieces after the peak load was reached. In addition wood pieces attached to the bags on the long side came into contact with one another, the data therefore became unreliable and testing was stopped. Significant tearing was noticed after testing mainly along the middle of the bag, confirming a higher stress concentration occurs in this region. Recovery after loading was removed was calculated to be 27mm, which considering the vertical stress experienced and given bag material had been significantly torn is reasonable high.

6.3.3.2 Unstabilised 70gsm polypropylene earthbag

Failure of the 70gsm polypropylene earthbag occurred at a much lower vertical loads than other samples, which was to be expected given the bag material has a lower tensile capacity. Even at relatively low loads (<20kN) tearing around the seams along the short side of the bag was noticed. As with the 100gsm polypropylene eight earthbag stack the earthbags experience an initial compaction before the bag material is initiated and a linear force displacement relationship occurs. Again recording movement of the earthbags proved problematic, with movement of the wood piece attached to the second from bottom earthbag on the long side at 144mm total vertical displacement. Furthermore the transducer on bag number 4 ran out of travel around 153mm. Despite this, data up to failure load of the earthbags is reliable and will be used for comparison against theoretical models in §6.3.4. The testing did give an indication of a potential global shear band. After removal of loading a clear level change was noticed in the cross section of the earthbags (see Figure 22). Furthermore tearing of the earthbags occurred on the top and bottom faces of the earthbag along a diagonal through the stack, see Figure 20 and Figure 22.



Figure 22: Tearing of 70gsm polypropylene earthbags after compression test

6.3.3.3 Stabilised earthbag

As expected the stabilised earthbag stack experienced a higher load capacity than the unstabilised earthbags. Using equation (4.25) we can quantify the cohesion the cement provides. Firstly the vertical stress is calculated using theoretical bag dimension, given the data obtained from the transducers is inaccurate.

$$\sigma_v = \frac{157000}{265 \times 450} = 1.31N/mm^2 \quad (6.3)$$

$$c' = \frac{1.31 - \left(\frac{2(19.2)}{77} \times 2.611\right)}{2\sqrt{2.611}} = 0.01N/mm^2 \quad (6.4)$$

The measurements of lateral expansion of the earthbag were inaccurate because the stack underwent rotation, which meant initial measurements were recording the earthbags moving away from the transducers. The gimbal also was tilted during the test which may have caused and/or exaggerated the initial sway of the stack. Cracking was heard early in experiment, around 5kN loading. This is due to the cement bonds breaking from the sand, allowing the bag to deform. Initially the bags were not fully in contact with each other, given that they were rigid blocks of different dimensions. Hence, initially the stiffness of the stack is low as there are some gaps between the bags; the stiffness rises as the bags fully bear onto one another.

6.3.4 Comparison between experimental results with theoretical predictions

A summary of the results from the compression tests is given in Table 2. The displacement of the platen is divided by the number of bags to give the height of a single bag. Refer to Appendix B for initial bag dimensions and densities.

Table 2: Summary of earthbag compression test results

Ref:	Material / N° of bags	Bag weight (kg)	K _p	Bag failure load (kN)	x (mm)	Initial height of single bag (mm)	Height of single bag at failure (mm)
C1	100gsm PP / 3	20	2.53	190.7	28	105	96
C2	100gsm PP /3	15	2.61	206.7	24	86	78
C3	100gsm PP /5	20	2.53	139.0	46	100	90
C4	100gsm PP stabilised /8	20	2.61	157.0	79	87	77
C5	100gsm PP /8	20	2.53	128.8	115	110	96
C6	70gsm PP / 8	20	2.61	92.8	124	95	79

The compression test involving a hessian bag experienced complete collapse at 1755kN, however all tests involving single earthbags are unreliable due to end restraint effects. Evaluation of theoretical behaviour against actual behaviour will use data from the 8 bag stack compression test. Theoretical analysis will be made following the assumptions outlined in §4.1. The positions of the transducers for the tests are shown in Figure 20. Not all bags were measured therefore the assumption is made that all bags undergo a similar deformation. This is not true, and in some cases there was a large divergence between bag dimensions, however, for the purpose of the analysis this assumption must be made.

For theoretical analysis, it is assumed the earthbag remains in a plane strain condition throughout loading. From the measurements taken during testing as shown in Table 3 (short side displacement) it is clear this is not true. However, the magnitude of deformation is dependent upon which side of the bag the transducer positioned, i.e. if positioned on the folded end it will experience greater movement as the bag end can unravel. Secondly the wood pieces underwent some rotation throughout the experiment. For the stabilised test, a wood piece was not used for

the short side measurement and the transducer was positioned in the middle of the bag. As the stack underwent compression the transducer's position would have followed the curved edge of the bag, thus leading to a lower lateral displacement measurement to that which actually occurred. Measurements for lateral expansion of 'long side higher bag' in experiments C4 and C5 are inaccurate for reasons discussed in §6.3.3 so the lower bag data is used to calculate experimental widths in Table 3.

Table 3: Comparison between measured bag width with theoretical bag width at failure load.

Test	Short side displacement (mm)	Long side lower bag (mm)	Long side higher bag (mm)	Experimental width (mm)	Theoretical width <i>rectangular model</i> (mm)	Theoretical width, <i>semi-circular model</i> (mm)
C4	5.78	9.0	3.9	253	266	277
C5	7.16	8.4	2.7	247	264	289
C6	17.60	22.6	29.3	369	370	390

The theoretical width of an earthbag at failure is calculated from equation (4.2) and (4.17), for the rectangular model and semi-circular model respectively. The models use the assumed height of a bag given the displacement of the platen at failure from the experiments.

Figure 23 shows the deviation in volume of the earthbags from the original volume against displacement of the platen. From the graph it can be seen that all samples underwent an initial reduction in volume of similar magnitude. This was expected given the earthbags could never be fully compacted prior to testing. Figure 23 indicates that the stabilised stack underwent a high level of initial compaction, with relatively little lateral movement; the cause for this is discussed in §6.3.3. Up to the point of failure of the earthbags, the range of measured volume to initial volume was between 0.92 – 1.04. Given the issues raised regarding the accuracy of the transducer for test C4 and C5, measurements taken from transducer in C6 can be considered most accurate and these results deviate the least from constant volume, up to failure. Measuring the dimensions of earthbags prior to and during loading is an approximate process and therefore the data from testing must be taken with a reasonable margin of error. Thus, for the purposes of analysis and given the maximum deviation measured volume to initial volume is 8% it is fair to assume a constant volume throughout loading to failure of the earthbag.

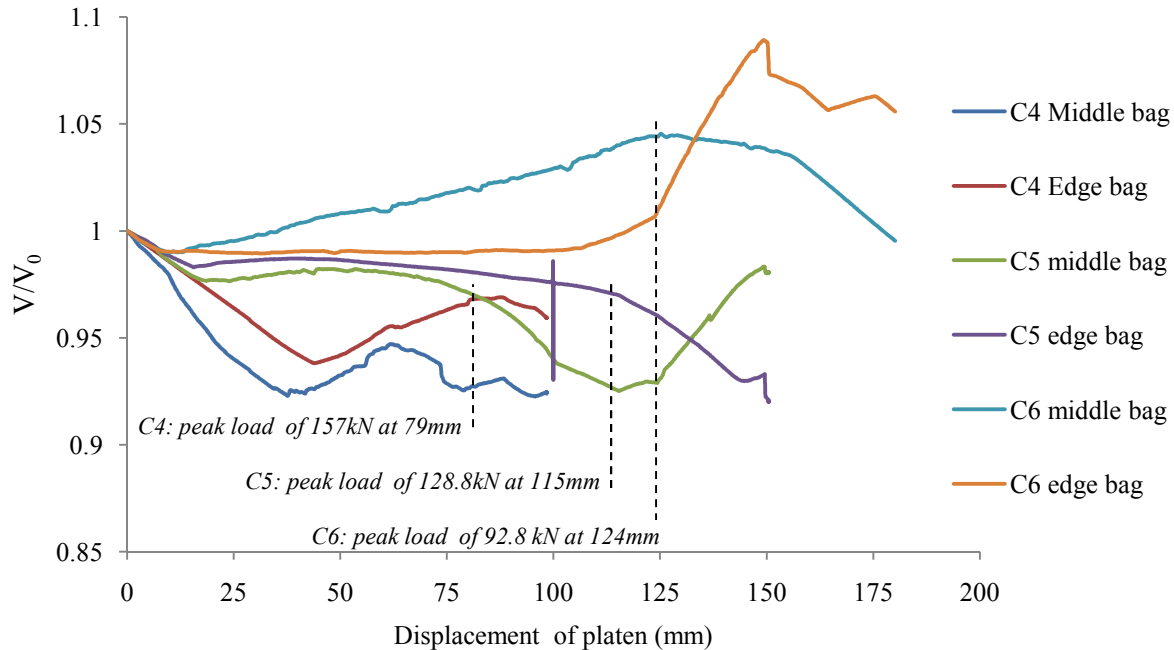


Figure 23: Ratio of measured volume of earthbag in 8 bag stack to initial volume of earthbag against displacement of platen

To calculate the theoretical vertical load applied to an earthbag to cause failure the value of x must be found using equation (4.7) assuming a rectangular cross section or equation (4.20) assuming a cross section with lateral semi-circular edges as discussed in §4.2.1. Taking the average values of E and σ_{bag}^{limit} found from the tensile tests and initial dimension of earthbags given in Appendix B, a value for x for individual bags is found to be:

Table 4: Comparison between theoretical vertical deformation and experimental vertical deformation of an earthbag.

Test	E (N/mm)	σ_{bag}^{limit} (N/mm)	Actual x (mm)	Theoretical x (mm) <i>Rectangular model</i>	Theoretical x (mm) <i>Semi-circular model</i>
C4	127.9	19.2	10.0	19.5	16.4
C5	127.9	19.2	14.4	28.2	22.3
C6	56.6	9.7	15.5	21.6	19.0

The theoretical models over estimate the magnitude of vertical deformation the earthbag has undergone up to failure. This is likely to be a result of an overestimation of the bag material strain capacity which could be due to an underestimation of the stiffness of the bag material or overestimation the tensile strength. The theoretical models only consider 2D confinement provided by the bag, in reality material fibres running longitudinally will act to resist lateral movement of the bag material and hence improve the stiffness of the bag. For a value of x , the strain experience by the bag material for the semi-circular model is higher than the rectangular, thus the rate of predicted tensile stress development in the bag material is higher. This is illustrated in Figure 44 (Appendix D). Hence with the semi-circular model, the tensile stress limit is reached at a lower value of x , which would produce a closer estimation of failure strength to

the experimental value. Using the experimental and theoretical values of x a predicted failure load for the earthbags can be made using equation (4.14):

Table 5: Comparison between theoretical and experimental failure loads of the earthbags under vertical compression

Test	Actual P_v (kN)	Theoretical P_v using experimental values of x at failure (kN)	<i>Rectangular model</i>		<i>Semi-circular model</i>	
			Theoretical P_v (kN)	$B_{failure}$ (mm)	Theoretical P_v (kN)	$B_{failure}$ (mm)
C4	157.0	155.2	202.5	303	185.3	290
C5	128.8	115.0	156.8	310	136.5	288
C6	92.8	85	99.6	401	93.1	388

The results show a good correlation between the experimental and theoretical failure loads calculated with a known value of x . For unknown value of x , assuming a rectangular cross section provides a grossly inaccurate prediction of the failure load of the earthbag for C4, a deviation of $\approx 30\%$ to the experimental result. The semi-circular model also overestimates the failure load (by 18%). It was thought both theoretical models would underestimate the strength of the stabilised earthbag, as they do not account for any initial cohesion provided by the cement which increases failure load as shown in Figure 9. The overestimation in strength could be a result of several factors; underestimation of E , overestimation of contact area at failure, overestimation of σ_{bag}^{limit} or inaccurate initial bag measurements. For the subsequent tests the semi-circular model provides reasonable predictions of the failure loads, thus can be considered a sufficiently accurate simplified analysis for the compressive capacity of earthbag under uniaxial compression.

6.3.5 Sources of error in experimental and theoretical work

Several sources of error for both the experimental and theoretical work have been explored, below is a summary of the key points:

- *End restraint effects*; as previously mentioned, frictional forces arise between the bag and the plates which oppose the lateral spread. Work is done to counter these forces and thus leads to inaccurate value of vertical stress.
- *Frictional forces will vary across the section*, maximum at the edges and minimum at the centre, hence barrelling of the earthbag.
- *Stress ratio is not constant*; during loading the density of the sand increases which will result in an increase in the friction angle and hence the value of K_p will rise.
- *Changing voids ratio*; all models assume a minimum possible voids ratio for the sand prior to loading, which is not true as the sand underwent some compaction during the early stages of loading. This is represented in Figure 44 by an initial negative region of $\Delta L/L_0$. Furthermore this assumption suggests once loading is started tensile forces in the bag material are initiated immediately. This could lead an underestimation of failure load; however, due to other affects, failure loads are generally overestimated even when end restraints effects are minimum.

- *Only 2D action considered in theoretical models*; the models only considers σ_1 and σ_3 they ignore σ_2 . Longitudinally confinement provided by the bag material is ignored.
- *Plane strain does not hold*. This is largely dependent on initial arrangement of bags as previously mentioned. However, in cases were the end did not fold out the bag still experienced longitudinal expansion. The assumption of plane strain is more realistic as the ratio of $l_0/B_0 \rightarrow \infty$. In an earthbag structure, the plane strain can be assumed as the bag will be restrained by neighbouring bags.
- *Inaccurate measurements of earthbags*; measurements of initial dimensions of earthbags are never 100% accurate due to the uneven shape of the bags. Furthermore recording deformations of the earthbags during testing proved problematic due to rotations of wood pieces and rotation of bag stack.

6.3.6 Summary and conclusion of compression tests

Predictably the bag material strength was the principal material aspect governing the strength of the earthbags. The 100gsm polypropylene earthbags were found to have the highest strength and were the easiest to construct with. Although hessian bags are not susceptible to UV degradation, which is a durability concern of polymer bags, they proved difficult to manage and failed during the single bag compression tests. Due to their fibre spacing, tamping of the bag resulted in a significant volume of sand escaping. The addition of 4% cement increased the load capacity by 22%; it also improved the stiffness of the earthbags which had a significant benefit for the arch tests, see §6.5.1.2. With regards to the testing procedure, the stack had a dramatic effect on the observed failure load of the bags. To reduce end restraint effects, a height to width ratio of $H_0/B_0 \geq 3.0$ is required, higher than that suggested by Lohani *et al.* (2006) ($H/B \geq 2.0$).

The assumption of constant volume of the earthbag for analysis can be considered to be acceptable up to failure of the earthbag, there after the assumption does not hold. Assuming a plane strain condition does not hold for unconfined compression tests, however, the theoretical models often overestimate the increase in width of the earthbag during loading by ignoring any initial compaction of granular particles. Therefore, this overestimation in width is somewhat offset by assuming plane strain, for the calculation of vertical failure load. Without assuming plane strain a more complicated 3D analysis would be needed, furthermore in practical application, the earthbags are restricted longitudinally.

The semi-circular model provided a more accurate theoretical model for the behaviour of earthbag under vertical compression. The accuracy of either model is subject to accuracy of initial measurement of earthbag dimension and bag material properties, thus the theoretical models must be taken with a reasonable margin of error. It is unlikely the vertical loads which the earthbags were subjected to during testing will be experienced during their structural lifespan. The compressive strength of a 100gsm polypropylene earthbag was found to be 1.7N/mm^2 . Overall deformations due to self weight are expected to be small. For example, assuming a 3.5m high unstabilised 100gsm polypropylene earthbag wall, bag height of 0.1m and

bag weight to be 20kg the lowest bag will experience a load of 6.9kN, from experimental data this would result in 1.8mm vertical deformation.

6.4 Shear Test of Earthbags

Large scale direct shear box tests between 20kg earthbags were performed as outlined in §5.4. From the experiments a relationship between shear stress / normal stress and horizontal displacement can be obtained. This data is displayed in Appendix C, which is used to calculate the residual shear stress / shear strength for each experiment. From the τ_f/σ_N against horizontal displacement graph a data range was selected where the ratio of τ_f/σ_N remained relatively constant. From this data range an average value of τ_f and σ_N was obtained; where more than one test was undertaken for a particular normal load an average was taken. The results for each of the experiments are represented in Figure 24. Graphs of τ_f/σ_N against horizontal displacement for all tests is given in Appendix C.

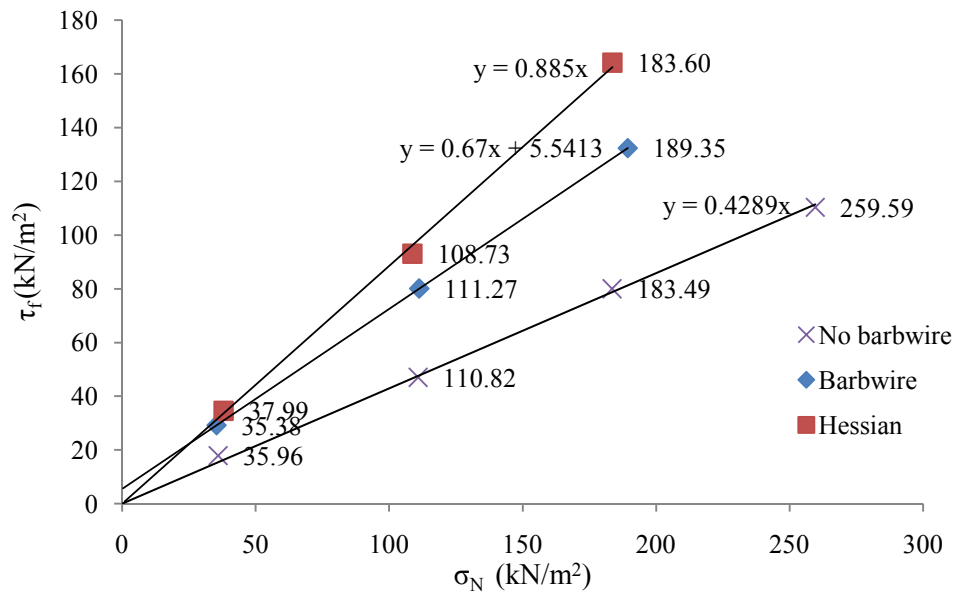


Figure 24: Shear strength against normal compressive stress for large shear box experiment with variation in interface between earthbags.

Table 6: Horizontal displacement at which shear strength was mobilised.

Test	Expected normal load (kN)	Average shear stress (kN/m ²)	Mobilisation (mm)	Friction coefficient μ
100gsm polypropylene no barbwire.	2.2	17.9	1.1	0.43
	7.1	47.0	0.7	
	12.0	80.0	1.9	
	17.1	110.3	1.7	
100gsm polypropylene barbwire.	2.2	29.2	11.7	0.67
	7.1	80.1	20.5	
	12.0	132.4	14.0	
Hessian no barbwire	2.2	34.6	7.4	0.89

	7.1	93.1	18.5	
	12.0	164.2	16.0	

- i) Initial density of earthbag: 17.6 kN/m³
- ii) Contact area taken as 0.066m²

The friction coefficient between the earthbags is obtained from the gradient of the linear regression of the points in Figure 24. For the hessian and no barbwire data the linear regression is forced through the point (0,0). It should be noted at low normal compressive stresses the accuracy of the results reduces. Furthermore providing a constant normal compressive force using a hand operated hydraulic jack system proved difficult at low loads. In addition the earthbags experienced dilatancy which caused the steel plate to tilt resulting in an increase in normal load to try and sustain the vertical position of the plate. The tilt of the plate became significant with relatively large horizontal displacement hence the measured vertical position of the earthbags is inaccurate near the end of the test.

The graphs of τ_f/σ_N against horizontal displacement in Appendix C show good repeatability for shear tests without barbwire between the earthbags. Data for shear test with barbwire is more wide-ranging, as seen in Figure 41, which indicates the variability the barbwire brings to the interface.

As predicted the hessian bags provide the highest frictional resistance against sliding between two earthbags. It was noticed, after the experiment, that the interface between the bags included sand and water which had been forced out from the hessian bags due to the applied normal load. It is thought that the sand contributed to the high coefficient of friction obtained from the results.

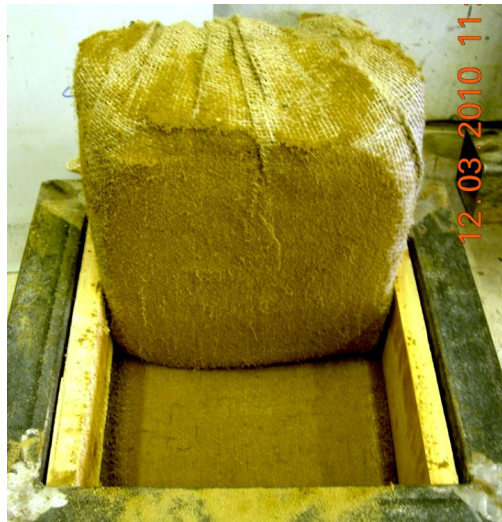


Figure 25: Interface between hessian earthbags after large shear box test

The two strands of 3-point barbwire between the earthbags provided an initial ‘cohesion’ of 5.54kN/m² and, unexpectedly, were shown to improve the friction coefficient between the bags. It is through that an increase in vertical stress increases the horizontal confining stress within the sand, thus the effective resistance provided by the barbwire points enhances resulting in a higher

friction coefficient between the bags. The linear regression for the polypropylene bags without barbwire actually provided an initial cohesion of 2.3kN/m^2 , but has been forced through the point (0,0) due to the unreliability of data at low applied normal loads. Hence, it can be seen that the cohesion provided by the two strands of barbwire was by no means substantial.

The improved shear strength provided by the barbwire strands is dependent on several factors namely, length of barbwire point, orientation of barbwire point, density of soil, soil bearing strength and stiffness of barbwire. How the barbwire is initially laid between the earthbags is an influential factor on the shear strength between the bags. For this experiment attention was paid to ensure the barbwire points penetrated the earthbag material, however, during construction of earthbag structures this is easily neglected, therefore the effectiveness of the barbwire is reduced. The use of barbwire is beneficial during construction as it provides an apparent cohesion between the bags which resists shear forces generated from tamping the earthbags, thus preventing the earthbags sliding due to this action.

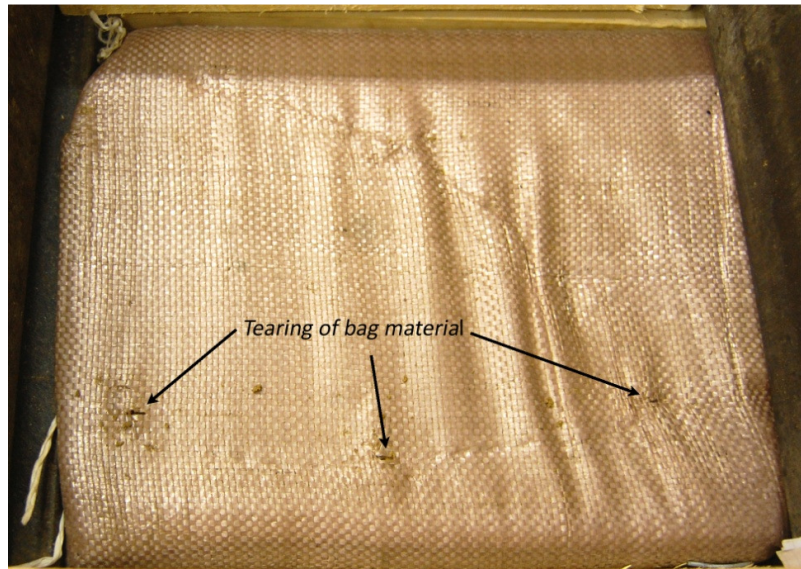


Figure 26: Photo of earthbag showing points where bag material was torn during direct shear test.

A small amount of tearing around the barbwire point on the lower bag was noticed after the experiment, see Figure 26. Therefore the barbwire point must have undergone translation as well as rotation failure. No significant tearing was noticed on the upper bag, given the bag remained stationary. Table 6 indicates that the shear strength mobilisation is much higher with barbwire and hessian bags than polypropylene bags; illustrating the addition of barbwire or use of hessian bags allows the earthbag to sustain higher shear displacements.

From the results of the shear box test, it was deduced that the failure mechanism for the barbwire arch would not be due to sliding. This can be supported by comparing the coefficient of friction

$\mu = 0.67$ to that of a traditional masonry on masonry system $\mu = 0.6 - 0.7$ (Cobb, 2009) which, for an arch of similar geometry, would fail due to formation of hinge mechanism.

6.4.1 Shear resistance in earthbag structures

As shown with the large shear box tests the barbwire increases the friction between the bags, however, there is a further resistance against an out of plane shear force provided by barbwire points which is detailed below. Consider an external line load acting on a proportion of an earthbag dome, as shown by Figure 27. It is thought the stiffness of the barbwire strand is significantly higher than the barbwire point. As the force pushes the bags inside the dome, the barbwire strand remains rigid and is pulled by the barbwire point within the earthbag subject to the external force undergoing translation. This in turn exerts a force onto the connecting earthbags' barbwire points neighbouring the earthbag subject to the external force. Translations of these barbwire points are resisted by the bag material and fill within the earthbag; this therefore acts to resist movement of the earthbag subject to the external force. For an internal applied load this component is initiated at small deformations, although would be small. However, for external loads acting on a dome structure, at small deformations no resisting forces are initiated given the barbwire strand would be in compression, see Figure 27. Resisting forces are activated once the angle between barbwire points, γ , is $\leq 90^\circ$, assuming a co-ordinate system as shown in Figure 27.

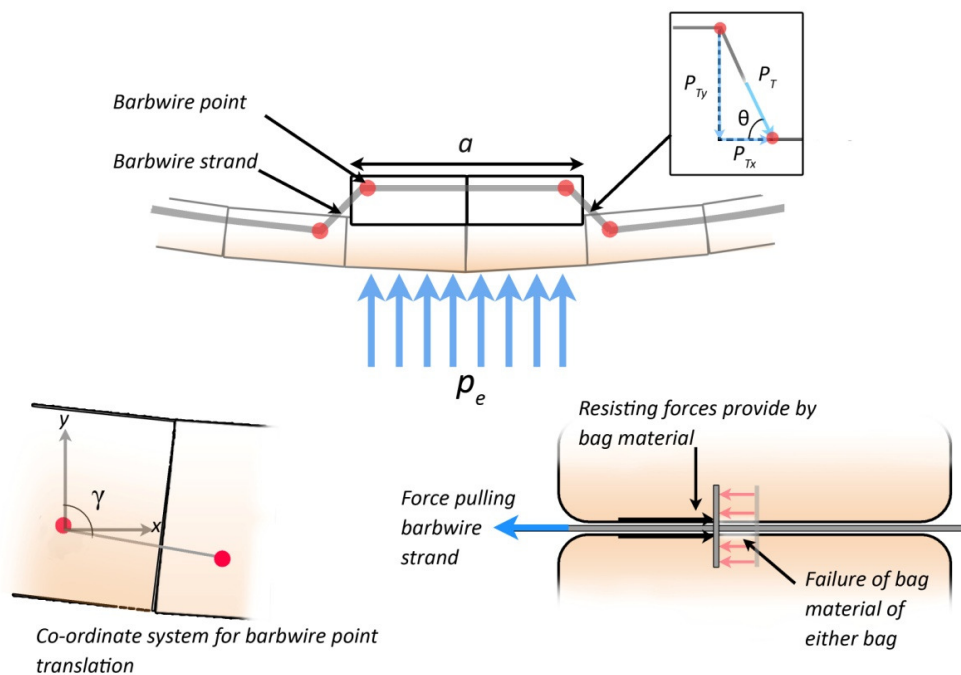


Figure 27: Predicted shear failure mode of earthbags in a dome structure subject to a line load.

$$p_e \cdot a = 2P_{Ty} \quad (6.5)$$

$$p_e \cdot a = 2(P_T \sin \theta) \quad (6.6)$$

For large values of a , the external applied force must be resolved perpendicular to the tangent of the dome.

A rough estimation of the required force to cause translation of the barbwire point, in adjacent unloaded earthbags can be made using the data from the large scale direct shear tests. From the tests the barbwire was found to provide an apparent cohesion. Given that with no applied normal load, the shear resistance between polypropylene earthbags is expected to be zero, one can deduce that this apparent cohesion is solely due to the effect of the barbwire. Thus from the apparent cohesion the maximum resisting shear force provided by the neighbouring earthbags due to the mechanism illustrated in Figure 27 can be estimated. However, for the shear tests, only tearing of one earthbag's wrapping material was experienced, whereas with the mechanism shown in Figure 27 failure of both earthbags' wrapping materials will occur. This can roughly be accounted for by multiplying the calculated resistance by two:

$$P_T = 2(\tau_f \cdot A) = 2 \times 5.54 \times 0.235 \times 0.453 = 1.18kN \quad (6.7)$$

This approximate estimation of the maximum resisting force is an overestimation of the actual resistance provided. Firstly the shear stress obtained from Figure 24 is a residual shear stress, thus this value is only achieved once a degree of translation of the earthbag occurs. For an external shear force this is less of a concern given the angle between barbwire points must be $\leq 90^\circ$ (see Figure 24), thus some initial movement is needed for a force to be initiated. Secondly the large scale direct shear tests used two strands of 3-point barbwire. Therefore the force calculated in (6.7) is the resistance provided by 12 barbwire points assuming 2 of the three points pierce the bag material. Even though an overestimated resistance is found, it can be shown, comparable to the resistance provided by friction between the bags this force is negligible. Resolving in the direction of the applied load, the shear resistance is therefore given by:

$$P_{Ty} = P_T \sin \theta = 1.18 \sin \theta \quad (6.8)$$

From Table 6 it can be seen that the maximum recorded mobilisation was 20mm. Assuming the earthbag subject to the applied shear force has undergone 20mm displacement parallel to the applied load, the initial angle between barbwire points in adjacent earthbags is zero and the distance between barbwire points is 100mm, θ can be taken as:

$$\theta = \tan^{-1} \frac{20}{100} = 11.3^\circ \quad (6.9)$$

Therefore, for this case, resolving in the direction of the applied load and ignoring normal loads and compression forces tangential to the sides of the earthbag, it is shown that:

$$p_e \cdot a \leq 2(P_{Ty}) = 2(1.18 \sin 11.3) = 0.46kN \quad (6.10)$$

Figure 28 compares this force with the resistance provided through friction between the bags in a hemispherical dome; explanation of the derivation of the graph is given in Appendix E. The

influence of the mechanism illustrated in Figure 27 only becomes significant around $\alpha = 30^\circ$. However, for the region of the hemispherical dome where $\alpha < 51.82^\circ$ (Heyman, 1977) compressive forces act within ring segments which will operate to resist shear movement of the earthbag. These forces will be of a higher magnitude than the resistance provided by the action shown in Figure 27. In addition, a rendered earthbag structure is likely to have chicken wire mesh on its outside and possibly on the inside, if rendered both sides. This will act to resist shear displacement of earthbags through bending, assuming it is adequately connected to the structure.

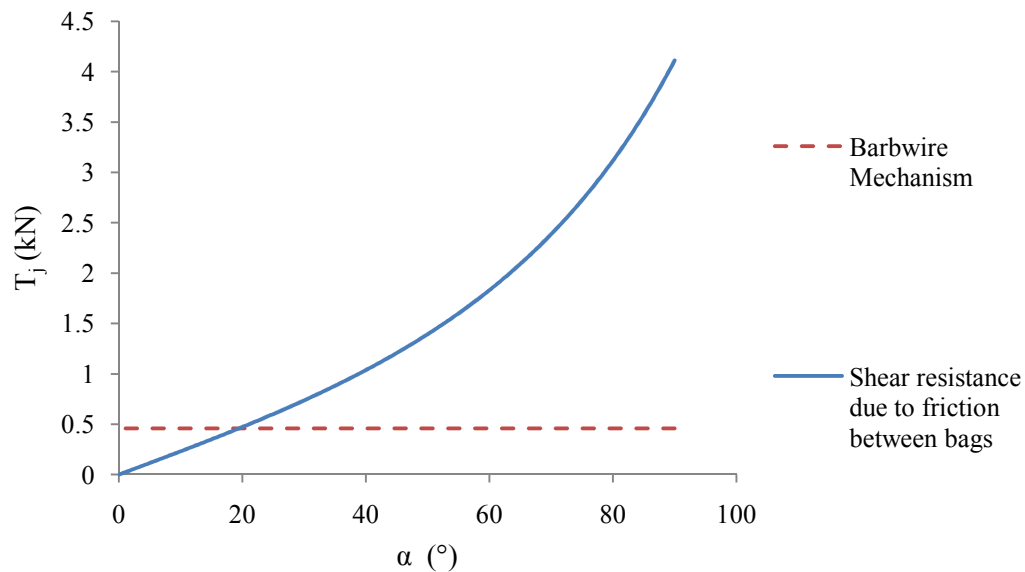


Figure 28: Comparison between shear resistance due to friction between earthbags and due to barbwire mechanism in a hemispherical dome.

Thus, it can be concluded that the principal mechanism of the barbwire in improving shear resistance between earthbags is individual dowel action of the barbwire points. Therefore, theoretically similar systems could be employed to provide adequate shear resistance between earthbags such as small wooden dowels/stakes, adequate diameter steel pins etc. Other forms of shear connections have previously been employed; Grasser & Minke, (1990) hammered bamboo poles through earthbags onto a continuous tie beam.

The advantage of using barbwire over other materials is that it can be easily sourced, quick to use and is cheap. On the other hand, as previously mentioned, the effectiveness of placing barbwire between earthbags to provide shear resistance is largely dependent upon the workmanship in forming the earthbag structure. Furthermore it can be somewhat difficult to handle and there is a safety issue both during construction and if it become exposed during the lifespan of the structure. The use of hessian bags would provide sufficient friction however; would not provide any initial cohesion. In addition hessian bags are very ductile therefore earthbag structures made with this material would be subject to higher deformations for relatively lower loads.

The importance of material factors in providing shear resistance is largely dictated by the geometry of the structure. That is to say, the issues regarding the shear resistance between earthbags becomes more prominent in wall or arch structures rather than a dome structure which is also less susceptible to disproportionate collapse.

6.5 Arch Test

Several arch tests were performed as outlined in §5.5 to gain a better understanding how earthbags behave in a structural sense and how the materiality affects the structural performance. Displacements of an arch were measured using transducers at quarter spans and mid span. Failure of the arch loaded at midspan occurred due to rotation of abutments; due to limited space in this dissertation this test will not be further discussed. In addition pictures of the arches were taken at various load increments and a continuous stream was taken during collapse of the arches. Pictures from the tests are put into a continuous video clip which is given in the accompanying C.D. The results of the tests are shown below:

Table 7: Summary of results from earthbag arch tests

Maximum load								
Test	N° of bags	Weight of arch (kN)	Vertical load (kN)	Horizontal load ^(c) (kN)	Quarter span (1) deflection (mm)	Midspan deflection (mm)	Quarter span (2) deflection (mm)	Stiffness of arch (kN/mm)
Unstabilised quarter span load – 2	28	5.35	4.12	1.53	41.8	-3.6	-12.6	-
Unstabilised midspan load	30	5.76	7.69	10.1	-16.7	64.3	-2.2	-
Stabilised quarter span load	30	5.75	7.26	3.36	8.75	-5.9	-1.3	1.32 (up to 4kN)
Barbwire quarter span load	29	5.71	3.85	2.50	40.4	-18.6	-8.4	-
Point of collapse of structure								
Test	N° of bags	Weight of arch (kN)	Vertical load (kN)	Horizontal load (kN)	Quarter span (1) deflection (mm)	Midspan deflection (mm)	Quarter span (2) deflection (mm)	
Unstabilised quarter span load - 1 ^(a)	23	4.38	2.0	1.2	17	-16	-15	
Unstabilised quarter span load – 2	28	5.35	2.32	1.44	89.5	-10.9	-25.1	
Unstabilised midspan load	30	5.76	5.59	8.27	-37.5	96.3	-4.2	
Stabilised	30	5.75	1.77	2.20	51.4	-34.9	-53.3	

quarter span load							
Barbwire quarter span load ^(b)	29	5.71	1.2	1.7	129.0	-55.8	-30.4

(a) Transducers were not used for this experiment, loading was read from load cells and measurements were taken from photographs.

(b) The displacements at collapse for the barbwire were measured from the pictures taken; the LVDT transducers were removed to protect them from the collapse of the structure.

(c) Includes thrust applied due to arch weight

6.5.1 Earthbag arches loaded at quarter span

6.5.1.1 Unstabilised no barbwire arch

An initial earthbag arch test was performed so an estimated failure load and deformation could be known. The failure load was measured as 2kN with a 17mm displacement underneath the applied load; it is clear this is much lower than the failure load for the second unstabilised arch test (4.12kN and 41.8mm). This difference can largely be accounted to improved initial compaction of the earthbags and an overall better constructed arch which meant a further 5 earthbags were needed for the test. This increase in bag number is also due to a slight increase in abutment spacing for the second test. During the first test it was noticed the earthbags did not fully bear onto the abutments, therefore were subject to rotation and thus not acting as fixity. From Figure 29 shows the earthbag is not fully supported, which meant the thrust line deviates from the arch at a lower loading. Experiment 2, unstabilised earthbag arch loaded at quarter span, will be used as a basis for comparison of material effects.

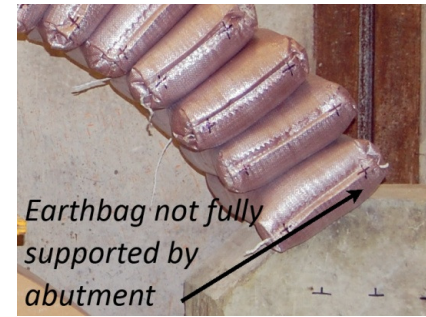


Figure 29: Picture of earthbag and abutment for first unstabilised earthbag arch test

Unload and reload cycles were performed on the arches to give an appreciation of the elasticity and recovery of the arch structure. Figure 32 shows the load displacement relationship at quarter span for the unstabilised earthbag arches loaded at quarter span. Full data up to collapse of the arches is not shown in this graph for clarity of the initial behaviour up to ultimate strengths. Unload reload cycles occurred around 0.5kN, 2kN and 3kN for the unstabilised no barbwire arch. The unstabilised arch with no barbwire had a low stiffness and showed little elastic behaviour. For 2kN applied load the arch experienced quarter span, mid span and three quarter span deflections of +13.9mm, +0.9mm and -2.6mm respectively. Therefore the arch has failed in serviceability at this stage, taking an allowable span to depth ratio of 1:200. In addition the arch showed little recovery which would be problematic for its practical application, e.g. for a similar span to rise ratio arch or open ended barrel vault structure.

There was no clear defined 4 hinge mechanism, however, near collapse of the arch some rotation between earthbags was beginning to form. Collapse of the arch occurred due to sliding between segments of the arch. The formation of a defined hinge mechanism could not occur because the earthbags did not behave rigidly, but that is not to say a mechanism did not form, merely that it was unclear. It is thought as the thrust line deviates from the centre line of the arch, rotation of the earthbags occurs. This reduces the contact area between the bags, which results in higher stresses acting between the bags. These stresses causes failure of the sand which redistributes within the earthbag to areas under lower stress, hence, the gap between the bags diminishes such that any initial rotation is reduced. Consequently, the arch has undergone deformation and the position of the thrust line must alter according to the new shape. Thus, overall, the behaviour of the arch is non-linear, which is support by Figure 32. The plastic analysis outlined in §4.4 assumes the earthbags do not fail in compression, which holds, however failure of sand does occur which reduces the accuracy of the analysis method.

6.5.1.2 *Stabilised arch*

The effect of having rigid earthbags can be seen by comparing the stabilised and unstabilised arches. The addition of 4% cement improved the ultimate strength of the earthbag arch by 76%. Comparing the behaviour of the two arches it can be seen that the stabilised arch experienced a sharp loss in load carrying capacity after peak ultimate strength, where as the unstabilised arch showed a more gradual reduction in load carrying capacity after ultimate strength.

The addition of cement meant the earthbags behaved more like rigid blocks, therefore in regions of high moment stress resultants hinges formed which redistribute the bending moments across the structure. From the arch pictures and video stream, it can be seen that the sharp loss in load carrying capacity corresponds to the formation of a hinge underneath the applied vertical load. The hinge causes rotation to occur which lead to deformation of the arch as load is applied.

Unload and reload cycles were performed at 1kN, 4kN and 6kN vertical load. Initially the arch showed elastic behaviour, with virtually full recovery after 1kN unload reload cycle. Residual deformations at quarter span of 1.4mm and 2.5mm were recorded by the transducers at 4kN and 6kN unloading and reloading cycles. This is more encouraging for the application of earthbag arches. It can be argued the arch did not fail in serviceability for an allowable span to depth ratio of 1/300. It is clear, that with respect to the unstabilised arch, the behaviour of stabilised arch is similar to that of a masonry arch, which makes it somewhat easier to predict failure load.



Figure 30: Photos from stabilised arch test showing hinge mechanism failure of arch

Analysis using ‘Ring 2.0’ software has been undertaken to compare the theoretical failure load of a masonry structure with the experimental failure load of the stabilised earthbag arch. The analysis program suggests an equivalent masonry arch with the same dimensions would fail in sliding at 7.9kN applied vertical load taking $\mu = 0.43$. This further confirms that the stabilised earthbags undergo local deformation which prevents individual earthbags from sliding out. However, it was concluded from Pelly (2010) that stabilised earthbag arch could be analysed as masonry arches.

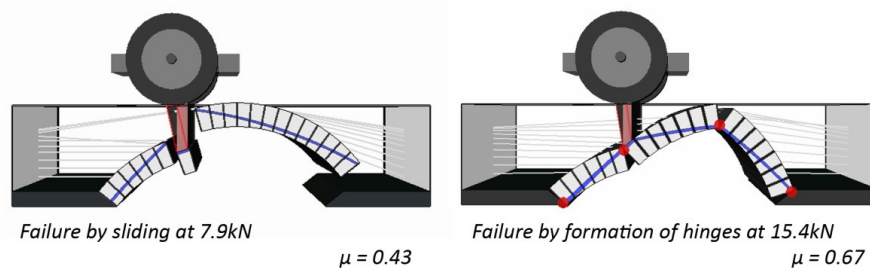


Figure 31: Masonry arch analysis using Ring 2.0

6.5.1.3 Barbwire arch

Like the unstabilised arch without barbwire a pronounced peak load was not achieved. The barbwire did not improve the strength of the arch; in fact the failure strength is slightly less than the unstabilised arch without barbwire. Up to 1kN applied load the behaviour of the arch was linear elastic, there after it was non-linear. Therefore the inclusion of barbwire prevented movement of the earthbags under relatively low loads. The arch was able to sustain a substantial deformation before collapse, around 39.5mm more at quarter span than the unstabilised arch without barbwire (measured from pictures taken during experiment). Although the arch was able to sustain loading at high deformation, such deformations are well above the acceptable limit for practical application. The structure would be designed such that failure strength is not reached. Therefore, it can be argued that the barbwire has no positive affect in this application given the arch structure without barbwire achieved a similar load capacity. However, the barbwire does

provide resistance against shear forces developing due to out of plane loading which must be consider in a practical application.

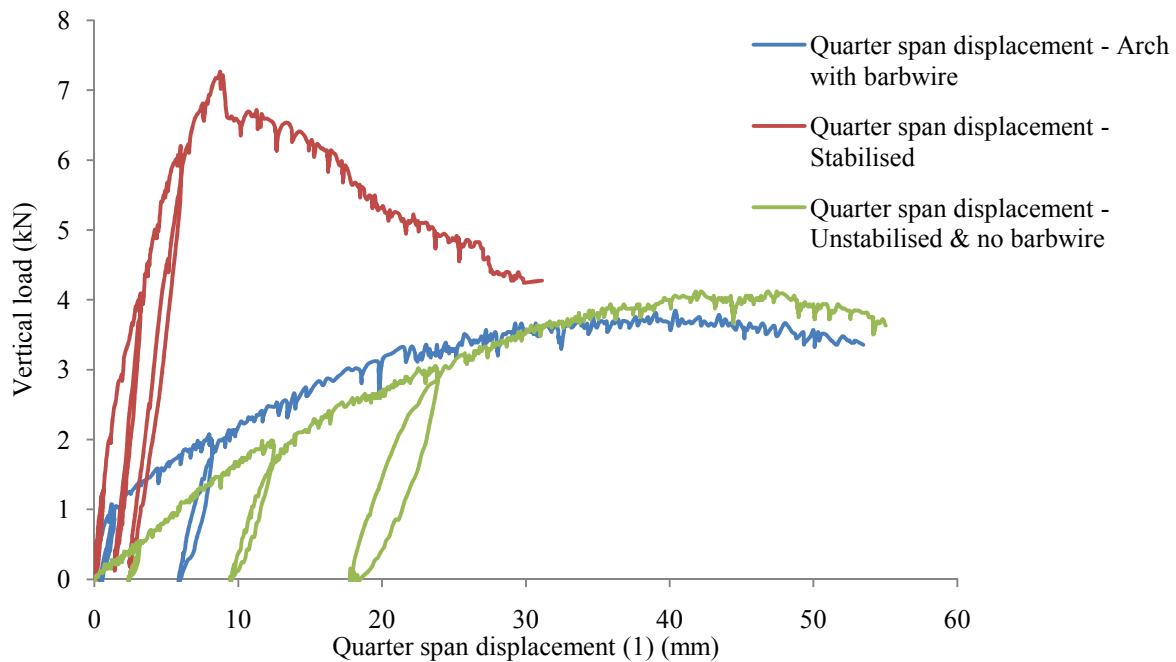


Figure 32: Load displacement graph for earthbag arches loaded at quarter span

6.5.2 Summary and conclusion of earthbag arch tests

It is clear from tests that the addition of 4% cement made a significant effect on the behaviour of the earthbag arch. The addition of cement caused the earthbags to behave as semi-rigid blocks, as follows, can be seen to act more like a masonry arch. A similar affect could be seen with the addition of clay content in improving the strength of the arch structure. The magnitude of improvement is largely dependent on percentage clay added and moisture content thus empirical analysis is required. Both the stabilised and unstabilised arches did not fail prematurely due to sliding. Therefore the addition of barbwire did not improve the failure strength of the arch, although increases its capacity to sustain higher deformations. However, the magnitude of shear stresses developing between the earthbags is a function of the geometry of the arch and applied load(s), thus the application of barbwire is geometrically dependent.

For the arches loaded at quarter span the hydraulic load ran out of travel, often prior to the arch reaching peak load. Additional wood / metal blocks were placed underneath the load, however, rotation of these blocks occurred which meant the load was not applied vertically to the extrados. This may have resulted in a lower peak load. Quality control on the construction of the arch is also a principal factor governing the load capacity of the structure; this is most evident when comparing the results from the first and second unstabilised arches without barbwire.

7 Conclusion

Experimental and analytical analysis on the behaviour of earthbags in relation to earthbag housing has been conducted. Particular focus has been paid to define material parameters required for the design of earthbag structures.

Compression tests on earthbags with variations in stack height, material fill quantity and bag material have been performed. The behaviour of an earthbag in compression is non-linear until the voids ratio of granular material reaches minimum, thereafter the load displacement relationship is linear almost to failure. The compressive strength of an earthbag is governed by several material parameters principally, tensile capacity of bag material, friction angle of soil and initial cohesion provided by soil. For an unstabilised 100gsm polypropylene earthbag the compressive strength was found to be 1.7N/mm^2 , hence compressive failure is unlikely to occur in an earthbag structure. However, unlike the polypropylene earthbags, the hessian earthbag failed under a single bag compressive test. The bag showed comparably less strength, was difficult to handle due to its flexibility and could not retain very fine sand. From testing, a stack height ratio of $H_0/B_0 \geq 3.0$ was found to be sufficient to minimise end restraint effects.

Analysis of compression data found that current theoretical models overestimate the vertical deformation of the earthbag up to failure leading to an overestimation of load capacity. A maximum divergence between measured earthbag volume and initial volume of 8% was found during testing to failure. Although measurement accuracy is suspect, deviation is not expected to be greater than 8%. Therefore, the assumption of constant volume is acceptable for the purpose of simplified analysis. A theoretical model assuming an earthbag cross section with lateral semi-circular edges was found to be most accurate in predicted the failure load.

Results from the large scale direct shear box tests between earthbags indicate the inclusion of barbwire improves the coefficient of friction and provides an initial cohesion between earthbags. The primary mechanism of the barbwire points in providing shear resistance is expected to be dowel action. Therefore, the effectiveness of the barbwire is dependent on density of granular fill, barbwire point surface area and orientation of barbwire point. However, this hypothesis should be further investigated through empirical analysis to confirm its accuracy. Hessian on hessian provided the highest coefficient of friction, however as before proved difficult to manage.

The addition of 4% cement produced a 76% increase in load capacity for the arch. With the addition of cement the earthbags behaved as semi-rigid blocks, with overall elastic behaviour up to 6kN applied load, and failure of the arch via formation of a defined hinge mechanism. The unstabilised arch did not fail prematurely due to sliding, owing to the flexible nature of bags, thus the addition of barbwire contributed little to the strength of the arch. Unlike the stabilised

arch both unstabilised arches failed in serviceability at relatively low loading. The quality control of construction was a significant influence on the failure load of the arches.

This work provides a preliminary investigation into the material and structural behaviour of earthbags. However, given the variable behaviour of earthbags with variation in structural system, continued research is required to gain an understanding on the structural limitations of earthbags. Some suggested further research areas are given below.

7.1 Future Work

The current structural form of most earthbag housing is a catenary dome; extrapolating data from the arch test to estimate failure strengths of a dome structure would provide very conservative answers. Thus full scale dome testing is required to quantify failure capacity and gain an understanding of how earthbags behave in 3d structures.

Often a barrier to the implementation of earthbag housing is its 'primitive' architectural form and departure from western buildings. Furthermore there are limitations to the use of earthbag domes for large scale projects. For the application of more orthogonal structures a greater understanding into the flexural strength of earthbag walls is required. A test procedure similar to that outlined in BS1052-2:1999 for determining the flexural strength of masonry walls could be implemented.

Other forms of shear connectors between earthbags should be investigated. A similar large scale shear box test as performed in this dissertation could be undertaken using wood dowels or steel pins between bags. The experiment would also verify whether the shear mechanism provided by the barbwire is primarily dowel action of the barbwire points.

The chosen materials which have been investigated in this project are limited specifically to relate to the Namibia project with FCBS. There is scope to investigate variation in soil constituents, specifically the addition of clay and how the variation affects the earthbag's behaviour.

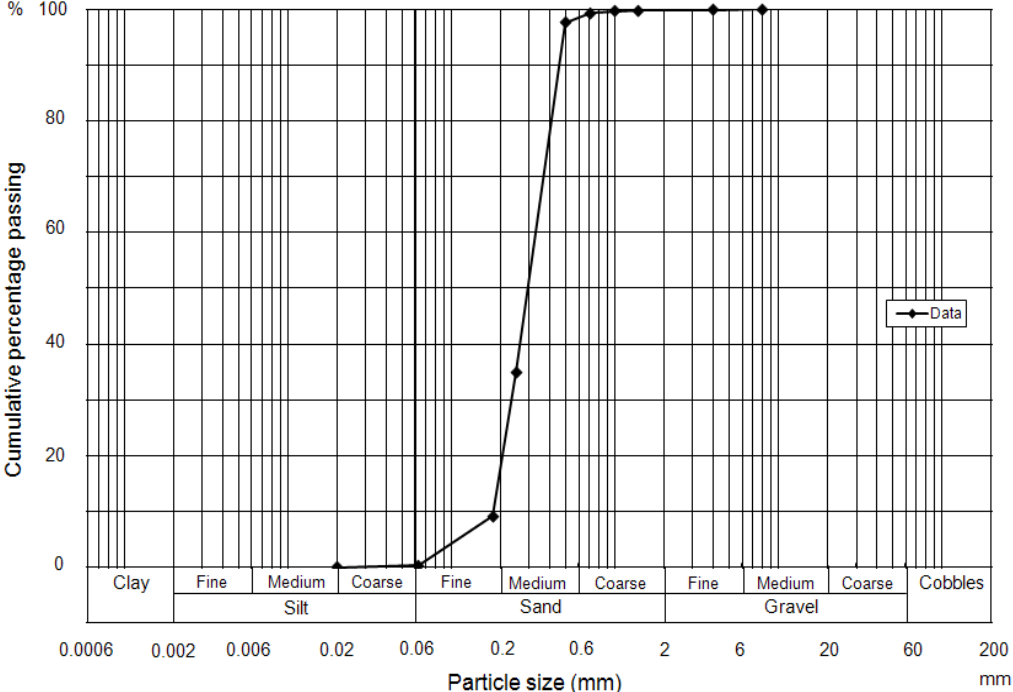
Finally, for the long term employment of earthbag structures, a further investigation into the material durability should be undertaken.

Bibliography

- Cal-Earth Inc. / Geltaftan. (2010, February 11). *Cal Earth photo gallery*. Retrieved March 29, 2010, from Cal Earth: <http://calearth.org/galleries/eco-dome.html>
- Broms, B. (1964). Lateral resistance of piles in cohesionless soils. *90*, pp. 123-155. *J. Soil Mechanics & Foundation Division ASCE*.
- BS1052-2:1999. (n.d.). *Methods of test for masonry. Part 2: Determination of flexural strength*. BSI.
- BS1377-2:1990. (n.d.). *Methods of test for Soils for civil engineering purposes. Part 2: Classification tests*. BSI.
- BS1377-7:1990. (n.d.). *Methods of test for Soils for civil engineering purposes -. Part 7: Shear strength tests (total stress)*. BSI.
- BS4102:1998. (n.d.). *Specification for steel wire for general fencing purposes*. BSI.
- Cobb, F. (2009). *Structural engineer's pocket book* (Second edition ed.). Oxford: Elsevier.
- Daigle, B. (2008). *Earthbag housing: Structural behaviour and applicability in developing countries*. Queen's University, Ontario, Canada, Department of Civil Engineering.
- DeJong, J., & Frost, J. (2002). Physical evidence of shear banding at granular-continuum interfaces. *15th ASCE Engineering Mechanics Conference*, (pp. 1-7). Columbia University, New York, NY.
- du Pisanie, N. (2009). Community building - Sustainable, appropriate desert building for the Topnaar communities of the Kuiseb River. *11th international conference on non-conventional materials and technologies*.
- Gilbert, M., Casapulla, C., & Ahmed, H. (2006). Limit analysis of masonry block structures with non-associative frictional joints using linear programming. *Computers and Structures*. (84), 873-887.
- Grasser, K., & Minke, G. (1990). *Building with Pumice*. Friedr. Vieweg & Sohn Verlagsgesellschaft.
- Heyman, J. (1977). *Equilibrium of shell structures*. Oxford University Press.
- Heyman, J. (1995). *The stone skeleton : structural engineering of masonry architecture*. Cambridge University Press.
- Huang, W., & Bauer, E. (2003). Numerical investigations of shear localization in a micro-polar hypoplastic material. *International journal for numerical analytical methods in geomechanics* (27), 325-352.
- Jewell, R. A., & Wroth, C. P. (1987). Direct shear tests on reinforced sand. *Geotechnique*, 37 (No. 1), 53-68.

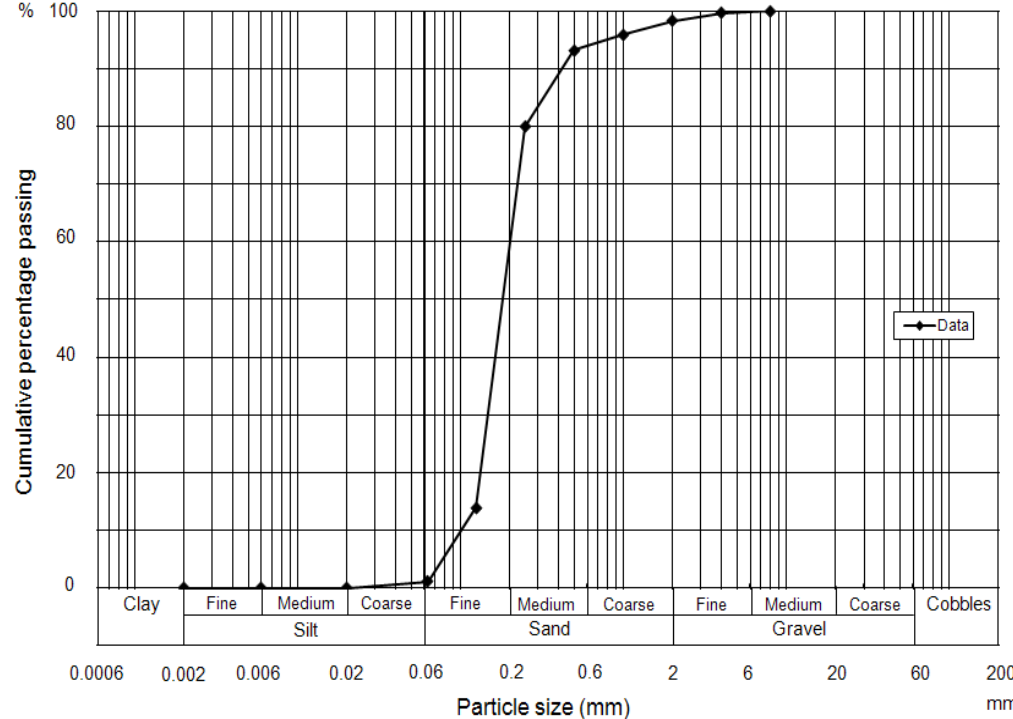
- Kibbert, C. (1994). Principles of sustainable construction. 1-9. Tampa, Florida, US.
- Koerner, R. (1997). *Designing with Geosynthetics* (4th Edition ed.). New Jersey: Prentice Hall.
- Livesley, R. (1978). Limit analysis of structures formed from rigid blocks. *International Journal of Numerical Methods in Engineering* (12), 1853-1871.
- Lohani, T., Matsushima, K., Aqil, U., Mohri, Y., & Tatsuoka, F. (2006). Evaluating the strength and deformation characteristics of a soil bag pile from full-scale laboratory test. *Geosynthetics International* , 13 (6), 246-264.
- Matsuoka, H., & Liu, S. (2003). New earth reinforcement method by soilbags ("Donow"). *Soils and Foundations* , 43 (6), 173 -188.
- Pedley, M. (1990). *The performance of soil reinforcement in bending and shear*. University of Oxford, Soil mechanics group.
- Pelly, R. (2010). *Plastic limit analysis of earthbag structures*. University of Bath, Department of Architecture and Civil Engineering.
- Roscoe, K. (1970). The influence of strains in soil mechanics, 10th Rankine Lecture. *Geotechnique* , 20 (2), 129-170.
- Tantono, S. (2007). *The mechanical behavior of a soilbag under vertical compression*. Graz Univerisity of Technology, Institute of Applied Mechanics.
- Xu, Y., Huang, J., Du, Y., & Sun, D. (2008). Earth reinforcement using soilbags. *Geotextiles and Geomembranes* (26), 279-289.

Appendix A



18/1/10

Figure 33: Dry sieve analysis of Kuiseb riverbed sand, near Gobabeb.



1/2/10

Figure 34: Dry sieve analysis builders sand - Bath

Bath sand description:
 Medium grained, clean, light / yellowish / yellow, rounded SAND.

Appendix B

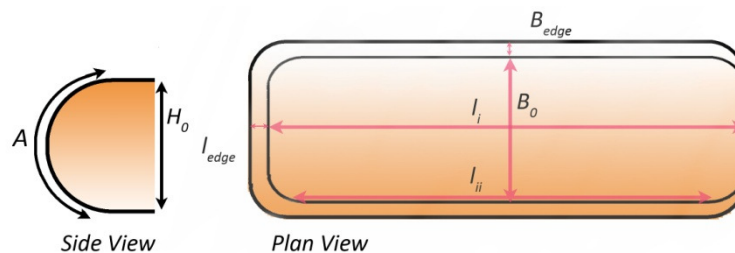


Figure 35: Diagram showing how earthbags were measured.

Table 8: Earthbag dimensions and densities for compression tests.

Experiment	Bag Material / Weight	l_i	l_{ii}	$l_0 = \frac{l_i + l_{ii}}{2}$	l_{edge}	B_0	B_{edge}	H_0	A	Volume (m^3)	Density (kN/m^3)
Compression test – 3bag	PP ₁ 10kg	340	310	325	18	280	18	68	93	7.15×10^{-3}	13.7
Compression test – 3bag	PP ₁ 15kg	410	337	374	25	230	28	86	118	8.55×10^{-3}	17.2
Compression test – 3bag	PP ₁ 20kg	480	425	453	35	235	30	105	130	0.013	15.1
Compression test – 3bag	PP ₂ 20kg	390	289	340	25	305	25	95	130	0.011	17.8
Compression test – 8bag	PP ₁ 20kg	430	410	420	40	230	30	110	150	0.013	15.1
Compression – stabilised test 8 bag	PP ₁ 20kg	470	430	450	10	235	10	87	100	9.80×10^{-3}	20.0
Compression test - 8 bag	PP ₂ 20kg	390	330	360	30	310	30	95	127	0.013	15.7
Arch test – ¼ span load	PP ₁ 20kg	412	360	386	25	212	25	100	171	9.68×10^{-3}	20.3
Arch test – barbwire	PP ₁ 20kg	480	445	463	35	235	35	103	100	0.014	14.6
Arch test – Stabilised	PP ₁ 20kg	480	440	460	35	250	35	101	100	0.014	14.6
Large shear box test	PP ₁ & H 20kg	-	-	300	-	220	-	110	-	0.0073	17.6

*PP₁ – Polypropylene 100gsm, PP₂ – Polypropylene 70gsm, H – Hessian. All bag dimensions are in mm unless stated. Date measurements were taken: Feb 2010 – April 2010.

Table 9: Moisture content of sand for barbwire and stabilised arch tests.

		Sample 1	Sample 1	Sample 1	Average
Arch test - barbwire	MC %	9.4	8.7	6.5	8.2
Arch test - stabilised	MC %	6.43	6.5	5	6.0

Samples were oven dried at 100°C for 24 hours.

Barbwire arch: 12/3/10 Stabilised arch: 1/3/10

Appendix C

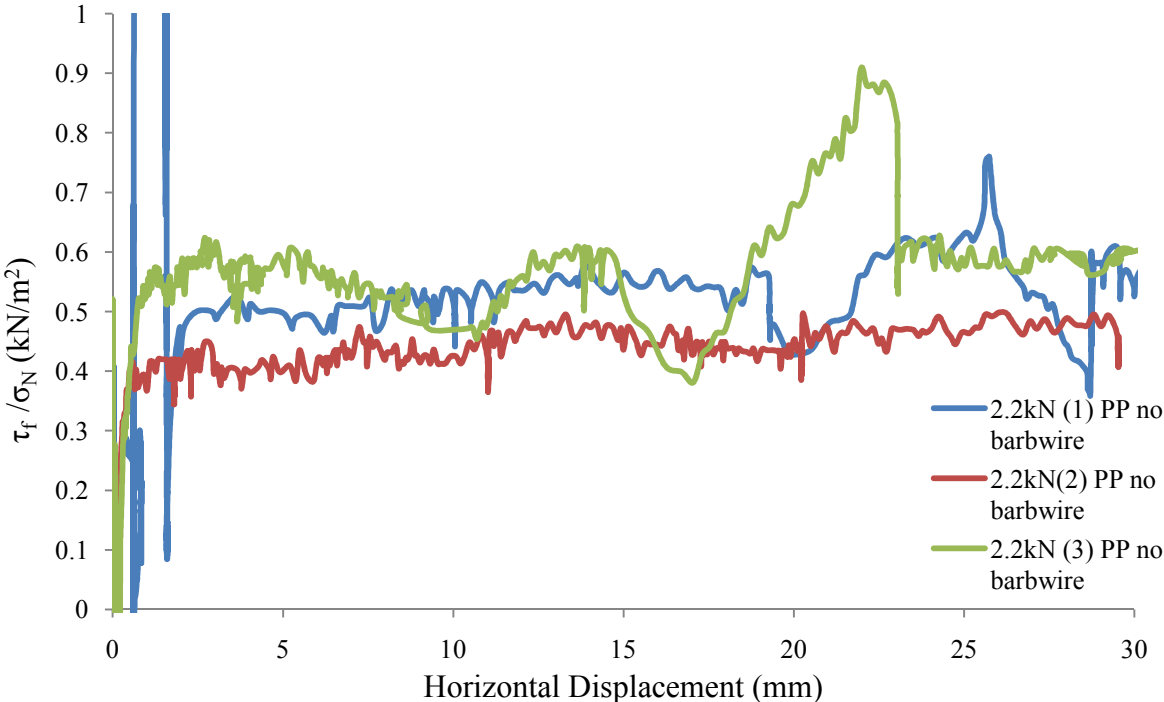


Figure 36: Large scale shear box test for 100gsm polypropylene earthbag no barbwire - 2.2kN applied normal load

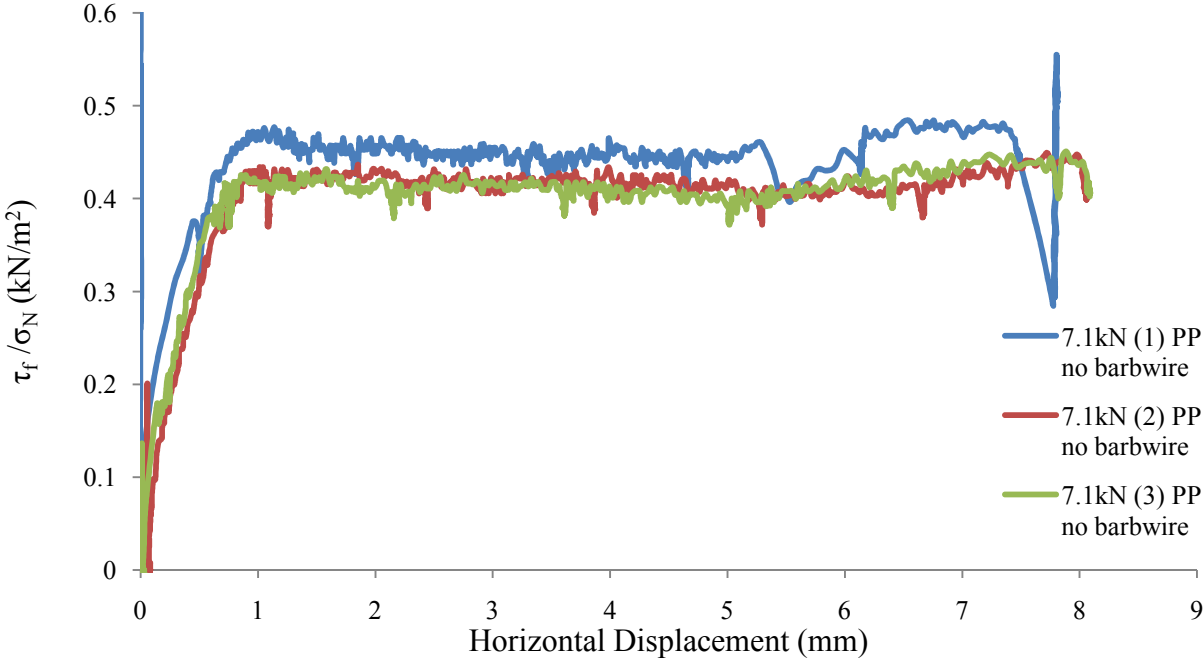


Figure 37: Large scale shear box test for 100gsm polypropylene earthbag no barbwire - 7.1kN applied normal load

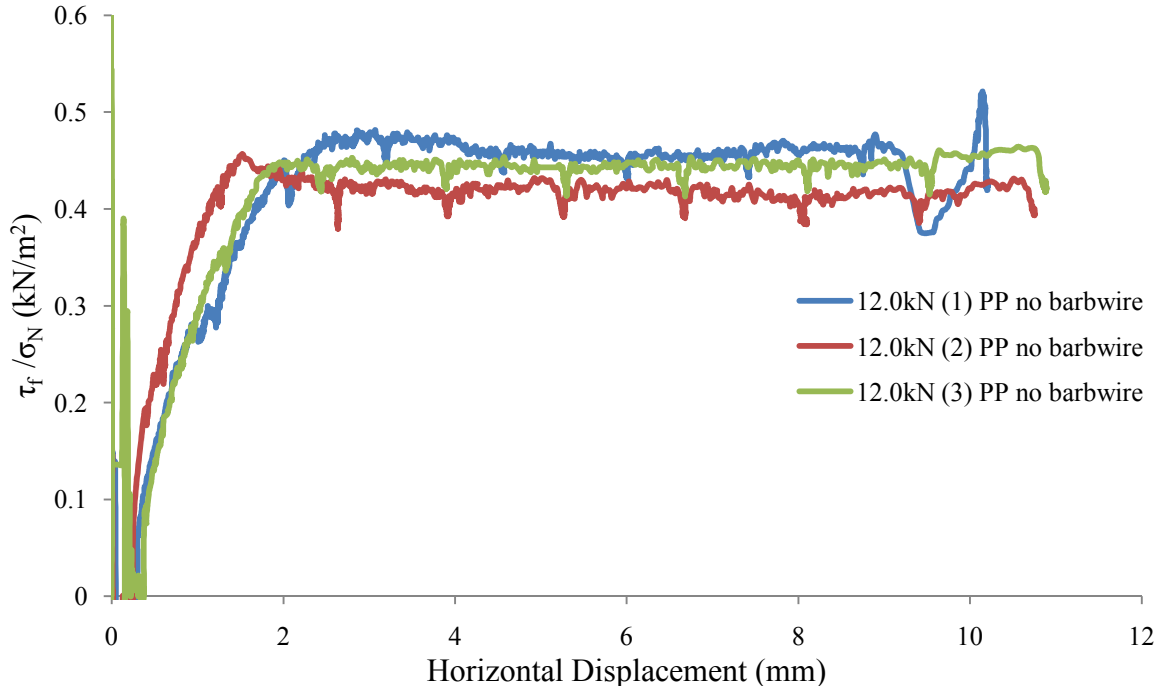


Figure 38: Large scale shear box test for 100gsm polypropylene earthbag no barbwire - 12.0kN applied normal load

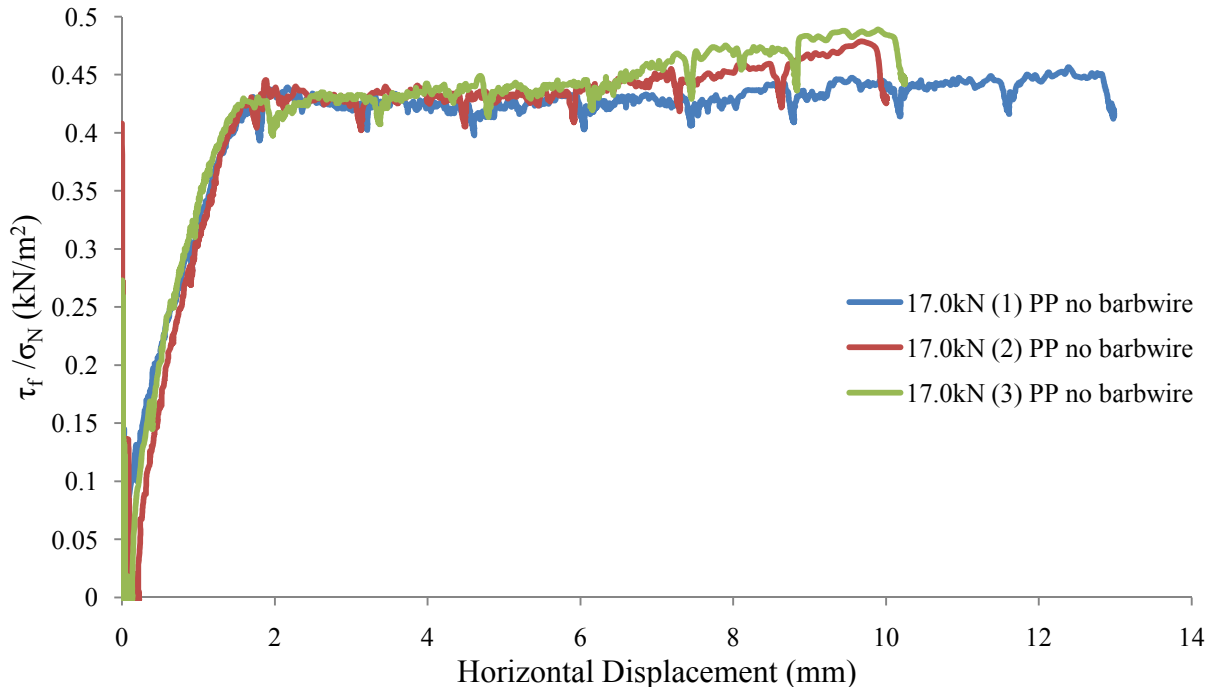


Figure 39: Large scale shear box test for 100gsm polypropylene earthbag no barbwire - 17.0kN applied normal load

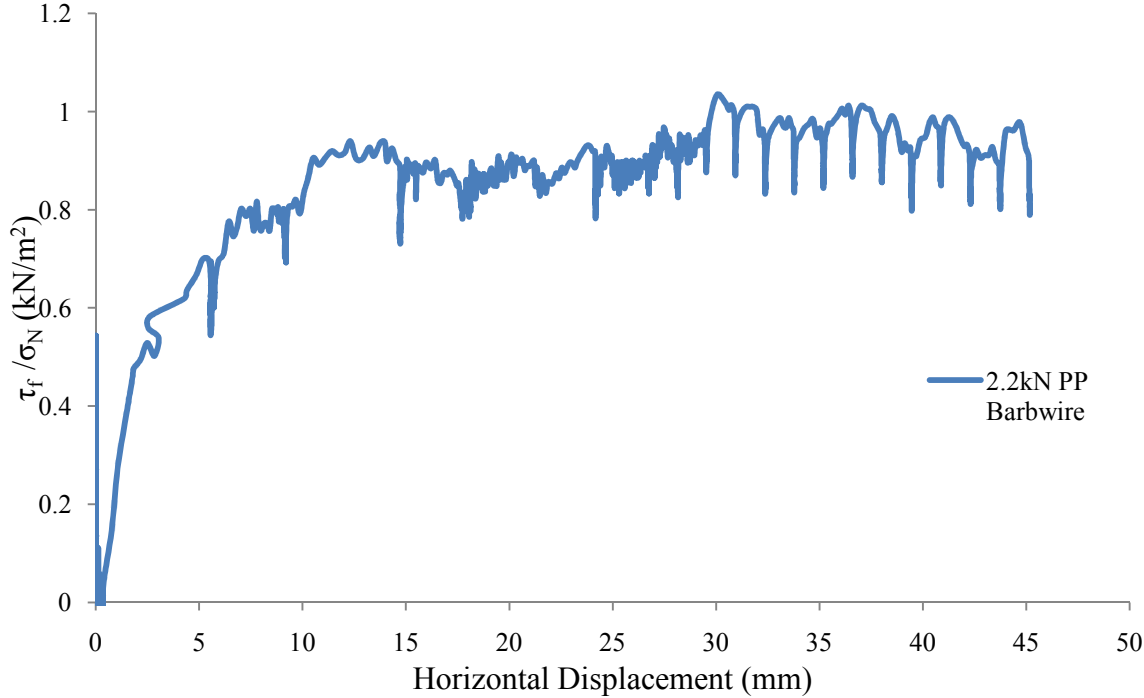


Figure 40: Large scale shear box test for 100gsm polypropylene earthbag with barbwire - 2.2kN applied normal load

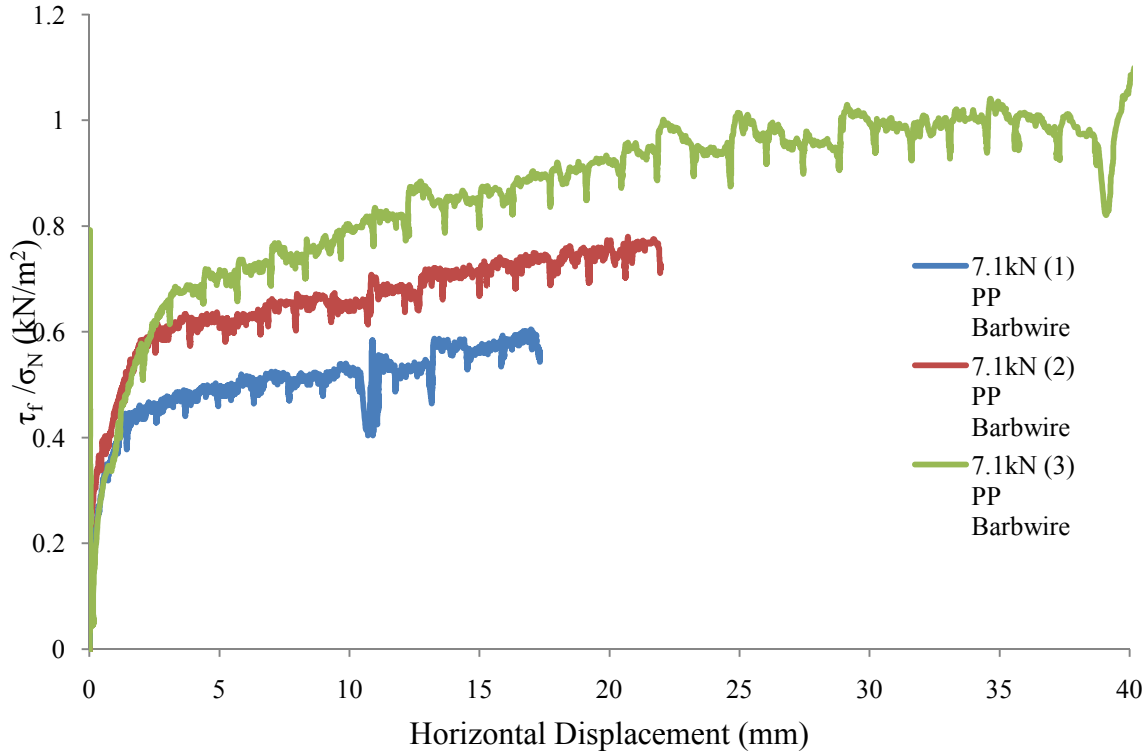


Figure 41: Large scale shear box test for 100gsm polypropylene earthbag with barbwire - 7.1kN applied normal load

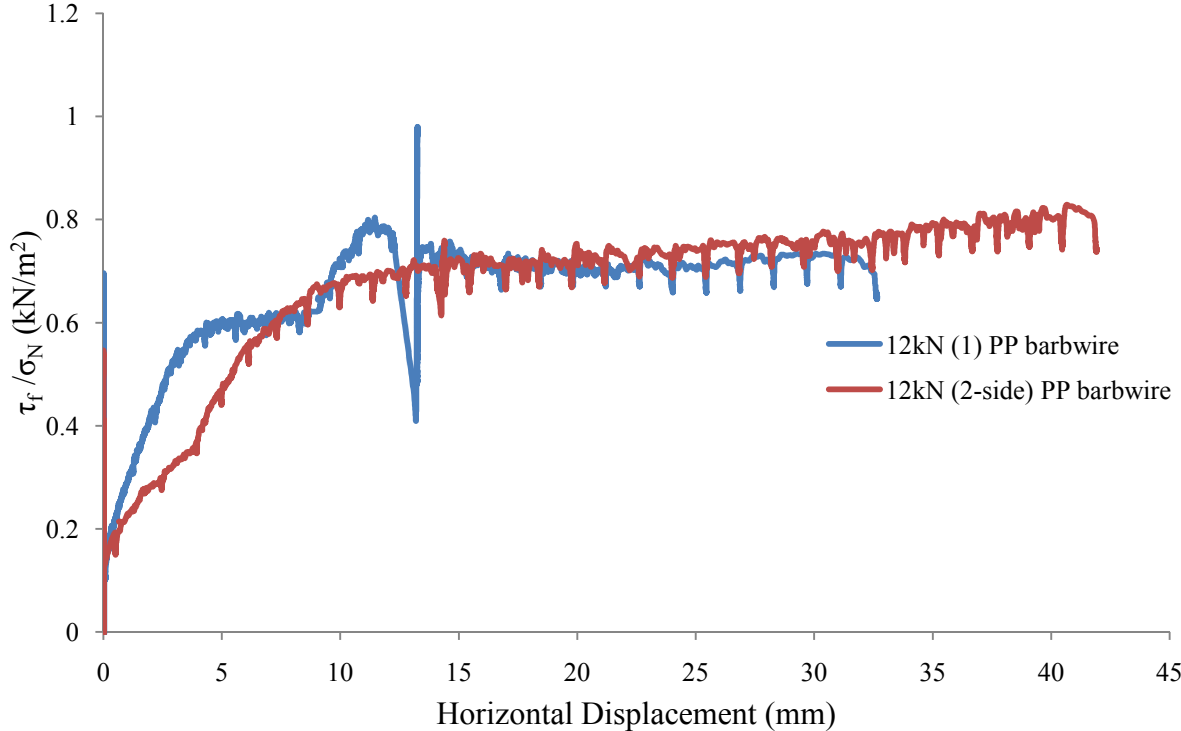


Figure 42: Large scale shear box test for 100gsm polypropylene earthbag with barbwire - 12.0kN applied normal load

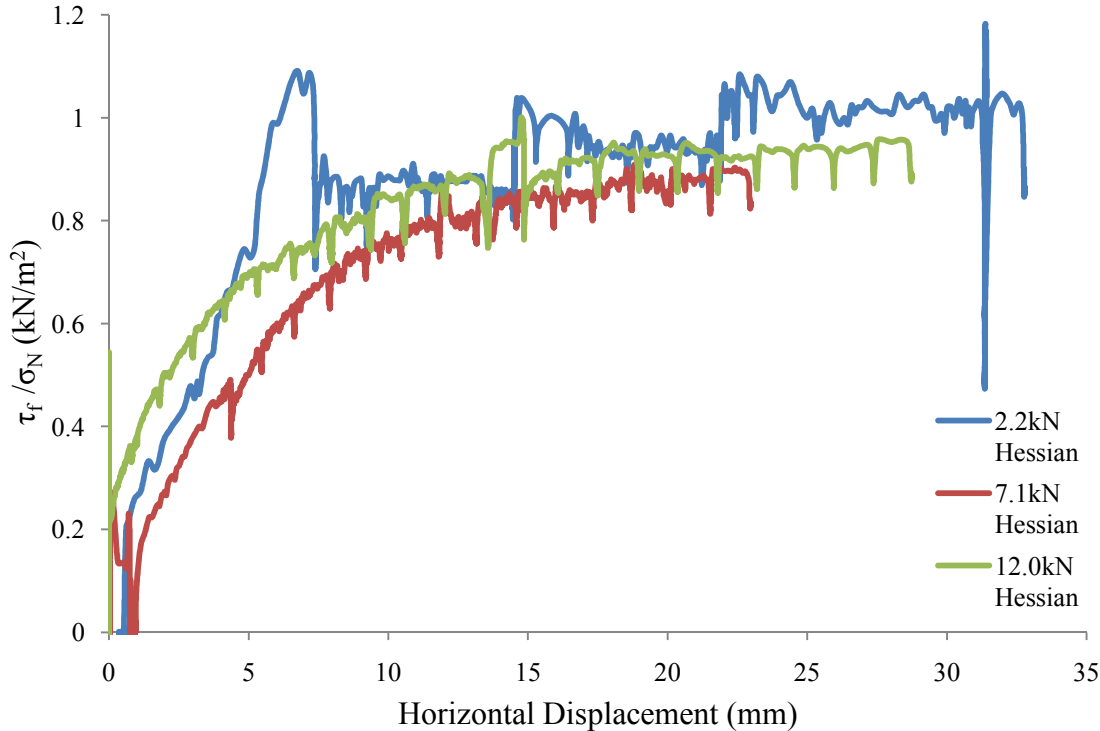


Figure 43: Large scale shear box test – hessian earthbags

Appendix D

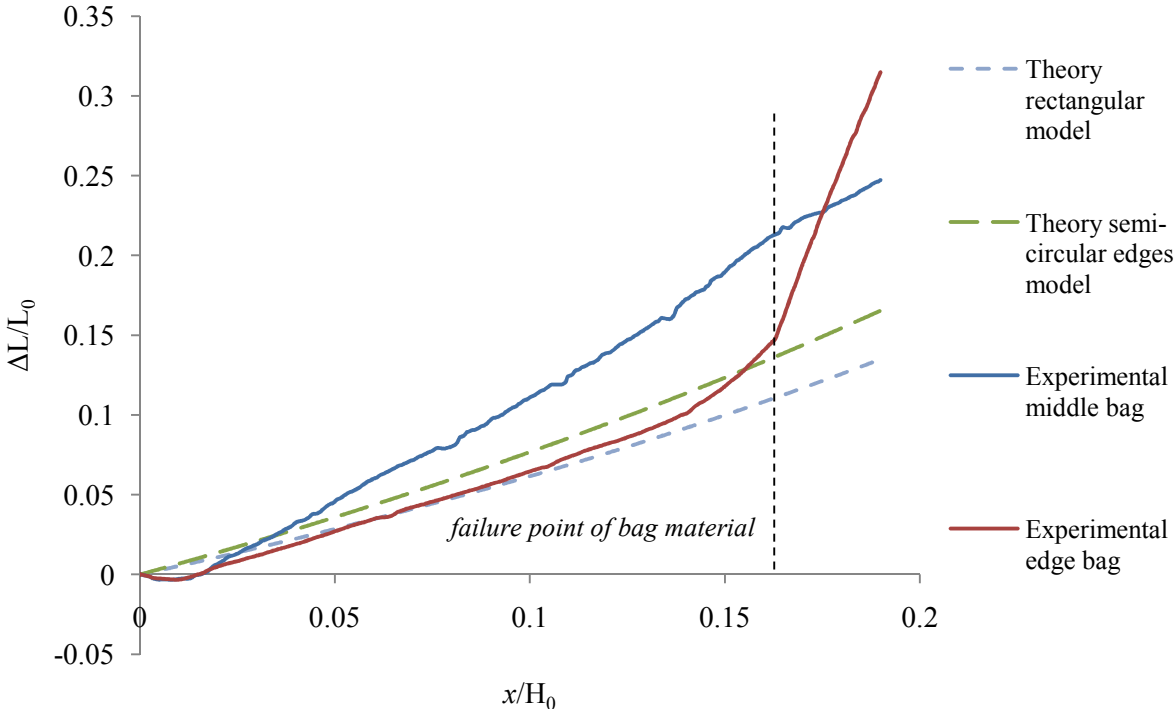


Figure 44: Change in perimeter over initial perimeter of 70gsm polypropylene earthbag in 8bag compression test against normalised displacement of loading platen

Appendix E

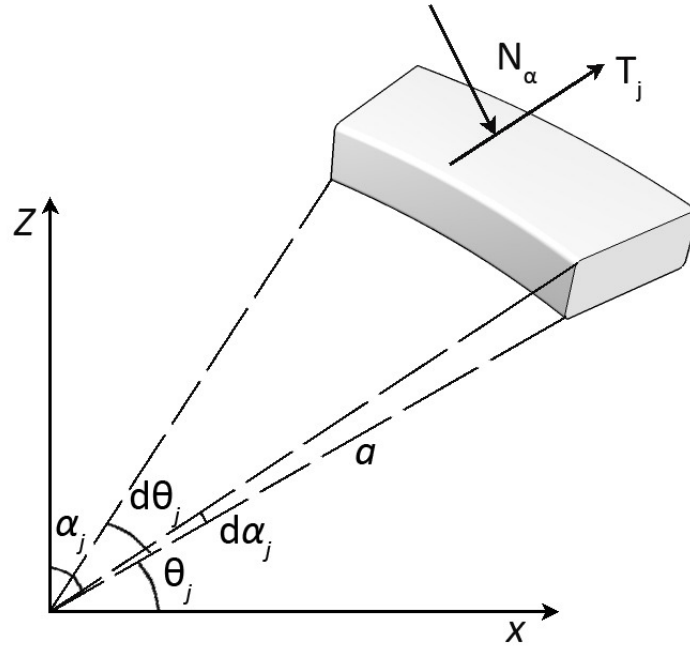


Figure 45: Single earthbag in hemisphere dome showing contact forces

The normal stress at the interface of a bag can be found from the co-ordinate system given in Figure 45, as shown by Heyman (1977):

$$N_{\alpha} = -\frac{wa}{1 + \cos \alpha_j} \quad (0.1)$$

Where w = density of earthbag material

The corresponding shear resistance is therefore:

$$T_j = N_{\alpha}\mu = -\frac{wa}{1 + \cos \alpha_j} \cdot \mu \quad (0.2)$$

The base of the dome is where $\alpha = \frac{\pi}{2}$; the initial segment length is taken as 450mm regressing to 0 at the top of the dome. The radius of the dome was taken as 3500mm, the earthbag width is taken as 230mm, coefficient of friction as 0.67 and the density of sand as 17kN/m³.